FACULTY OF PHARMACEUTICAL SCIENCES

Screening of pyrrolizidine alkaloids in tea matrices by IM-MS: first steps of method transfer to a user-friendly QqQ spectrometer for routine quantification

Marie Smet
Student number: 01900214

Supervisor(s): Prof. Dr. Chiara Dall'Asta, Prof. Dr. Marthe De Boevre, Dr. Raquel Torrijos

A dissertation submitted to Ghent University in partial fulfilment of the requirements for the degree of Master of science in the drug development
Academic year: 2022 – 2023

UNIVERSITEIT GENT

UNIVERSITÀ DI PARMA

ABSTRACT

Pyrrolizidine alkaloids (PAs) are toxins biosynthesised by plants. Exposure to these alkaloids, can cause chronic diseases like: hepatotoxicity and carcinogenicity. Ion mobility spectrometry (IMS) has risen as a powerful technique for both targeted and non-targeted screening. Nevertheless, this approach remains largely unexplored in food safety because of the lack of collision cross-section (CCS) databases. In present work, the first IMS-derived CCS database for the 35 EU-regulated PAs was created, supplied by two algorithms trained with machine learning. The CCS database provided an additional separation dimension for isobaric and isomeric compounds. Low prediction errors, confirmed the additional benefit of the CCS database.

A primary objective of this work, was to screen 15 different tea matrices for PA contamination. The samples were analysed using a Vion IMS QTOF Mass Spectrometer. The number of contaminated samples was remarkably high. 14 of the 15 analysed samples were positively screened for PAs. The significant outcome confirmed that the objectives of this master scription were valuable.

Seen the complexity of the available time of flight (TOF) method, the aim of this work was to transfer the protocol to a user-friendly triple quadrupole (QqQ) analyser, to perform routine quantification. This scription contributed to the first stages of development of a new UPLC-MS/MS protocol, using a QqQ analyser. The technique enabled simultaneous determination of 21 PAs in tea samples. The developed methodology applied mobile phases of water and methanol, both in addition of an acidic modifier. After several modifications, a segmented gradient with flattened slopes, achieved the best possible separation of the target compounds. A crucial problem encountered during development was the co-elution of isomeric alkaloids. 18 of the 21 PAs in the standard mixture were baseline separated within 25 min. Co-elution could not be avoided for the following isomers; lycopsamine, intermedine and senesivernine N-oxide.

The initial objectives of this scription have been achieved. The first ever CCS database was created for PAs. 15 tea matrices have been successfully screened using IMS QTOF mass spectrometry. Thereafter, the TOF method was transferred to a user-friendly QqQ protocol. Validation of this method is necessary in the future.

SAMENVATTING

Pyrrolizidine alkaloïden (PA) zijn toxinen geproduceerd door planten. Blootstelling aan deze alkaloïden kan chronische ziekten veroorzaken zoals: hepatotoxiciteit en carcinogeniteit. Ion mobility spectrometry (IMS), is een relatief nieuwe techniek voor zowel gerichte als ongerichte screening. Desalniettemin, wordt deze techniek slechts weinig toegepast binnen de voedsel veiligheid, door het tekort aan collision cross-section (CCS) databases. In deze scriptie, werd de eerste CCS database aangemaakt voor de 35 Eu-gereguleerde PAs, met behulp van twee machine-learning algoritmes. De CCS database zorgde voor een additionele scheidingsdimensie voor isomeren en isobaren. De lage prediction errors, bevestigden het voordeel van de CCS database.

Een eerste doelstelling van het werk, was het screenen van 15 verschillende thee matrices, voor PA contaminatie. De stalen werden geanalyseerd door een Vion IMS QTOF Mass Spectrometer. Het aantal gecontamineerde stalen was opmerkelijk hoog. 14 van de 15 stalen werden positief gescreend voor PA contaminatie. Deze significante resultaten bevestigden dat de doelstellingen van deze master scriptie waardevol waren.

Gezien de hoge kosten en complexiteit van de time of flight (TOF) methode, was de doelstelling om het protocol te transfereren naar een gebruiksvriendelijke triple quadrupole (QqQ) methode. Deze scriptie, droeg bij aan de ontwikkeling van een nieuw UPLC-MS/MS-protocol. De techniek maakte gelijktijdige bepaling van 21 PAs in thee mogelijk. De ontwikkelde methode paste mobiele fasen van water en methanol toe, met een zure modificator. Een gesegmenteerde gradiënt met afgeplatte hellingen bereikte de beste scheiding van de PAs. Een cruciaal probleem was de co-elutie van isomere alkaloïden. 18 van de 21 PAs werden binnen 25 minuten gescheiden. Co-elutie kon niet worden vermeden voor de volgende isomeren; lycopsamine, intermedine en senesivernine N-oxide.

De doelstellingen van deze masterproef werden bereikt. De eerste CCS-database werd aangemaakt voor PAs. 15 theematrices werden met succes gescreend door IMS QTOF-massaspectrometrie. Daarna werd de TOF-methode omgezet naar een gebruiksvriendelijk QqQ-protocol. Validatie van deze methode is noodzakelijk in de toekomst.

ACKNOWLEDGMENTS

By writhing the acknowledgments, I end an instructive and fascinating period. This Erasmus was a fantastic and unforgettable experience. I will forever cherish the memories and friendships I have made and the places I visited. This exchange helped me broaden my personal, social and scientific horizon.

First of all, I would like to express my greatest gratitude to Prof. Dr. Chiara Dall'Asta for giving me the opportunity to be part of her laboratory. I am grateful for her warm welcome at the University and the interesting project she offered me.

Secondly, a warm thank you to Prof. Dr. Apr. Marthe De Boevre, my promotor form the University of Ghent. I would like to thank her for the trust and for giving me the opportunity to carry out my master scription at the University of Parma, Italy.

A big thank you to post-doc Raquel Torrijos, for her daily guidance trough every step of this master scription. Thank you for your scientific advice, answering my questions, the useful remarks and believing in me. I could not have done this without you. I wish you a lot of success in the future and with your upcoming projects!

I would also like to thank the other PhD students and staff members for the pleasant atmosphere in the lab. Thank you for teaching me some Italian sacred culture and learning me to appreciate coffee, un grazie di cuore a tutti!

A special thank you to Valérie to accompany me during this adventure! We arrived as strangers but after these intense months, I am happy to call you a friend.

To my loving parents, for their unconditional support, for granting me the opportunity to study and pursuing my dreams.

Last, but not least, my boyfriend Tibo for supporting me to write this master scription abroad. Thank you for encouraging me through all the ups and downs the past four years. Even though you weren't there, our phone calls meaned a lot to me.

Thank you all.

TABLE OF CONTENT

ABBREVIATIONS

API	Atmospheric pressure ionisation
ARfD	Acute reference dose
At	Atropine
CCS	Collision cross-section
CE	Collision energy
CONTAM	Panel of contaminants in the food chain
EA	Ergot alkaloid
EFSA	European Food Safety Authority
EM	Electron multiplier
ESI	Electron spray ionisation
IMS	Ion mobility spectrometry
IM-MS	Ion mobility-mass spectrometry
LC	Liquid chromatography
LC-MS	Liquid chromatography- mass spectrometry
LLE	Liquid-liquid extraction
LOAEL	Lowest observed adverse effect level
LOD	Limit of detection
LOQ	Limit of quantification
MALDI	Matrix-assisted laser desorption ionisation
MOE	Margin of exposure

MS	Mass spectrometry
m/z	Mass-to-charge ratio
NOAEL	No observed adverse effect level
PA	Pyrrolizidine alkaloid
PANO	Pyrrolizidine alkaloid N-oxide
PTFE tube	Polytetrafluoro-ethylene tube
Q	Quadrupole
QuEChERS	Quick, easy, cheap, effective, rugged and safe
QqQ	Triple quadrupole
RASFF	Rapid alert system for food and feed
RF	Radiofrequency
RF	Reference point
RP-HPLC	Reversed-phase high pressure liquid chromatography
RS	Resolution
Sc	Scopolamine
SLE	Solid-liquid extraction
SMILE	Simplified molecular-input line-entry
SPE	Solid phase extraction
TA	Tropane alkaloid
TDI	Tolerable daily intake
TIC	Total ion chromatogram

TOF	Time of flight
TPP	Tetraphenyl porphyrin
UPLC	Ultra-high performance liquid chromatography
UV-vis	Ultraviolet - visible spectrophotometry
VOD	Veno-occlsive disease

1. INTRODUCTION

1.1. PLANT ALKALOIDS

1.1.1. General introduction

Every plant has a set of primary metabolites which are responsible for the vitality of the plant. These primary metabolites occur in every living cell and belong to the class of phytochemicals (1). Conversely, plant alkaloids are specialised secondary metabolites only present in the prominent tissues and necessary for specific functions of the cells (2). Alkaloids are stored in various cell tissues and released when the plant is exposed to environmental stress conditions. For centuries alkaloids have been used in traditional medicine to treat diverse ailments. During the last years, their toxic effects were more extensively studied. Alkaloid exposure can be dangerous and forms a threat to human health. Therefore, there is a need for better and faster routine analysis, to screen the possibly contaminated products (3). This way it can be prevented that alkaloid-containing products enter the market.

1.1.2. Function of alkaloids in the plant

Nitrogen is a characteristic element present in the chemical structure of alkaloids. Since nitrogen is one of the most important fuels of the plant, alkaloids are used to combat challenging and environmental stress conditions (4). Alkaloids are produced naturally as a reservoir to store nitrogen. Furthermore, these specialised metabolites are produced in varying levels in different parts of the plant (such as the roots, leaves, flowers, seeds and fruit) (5).

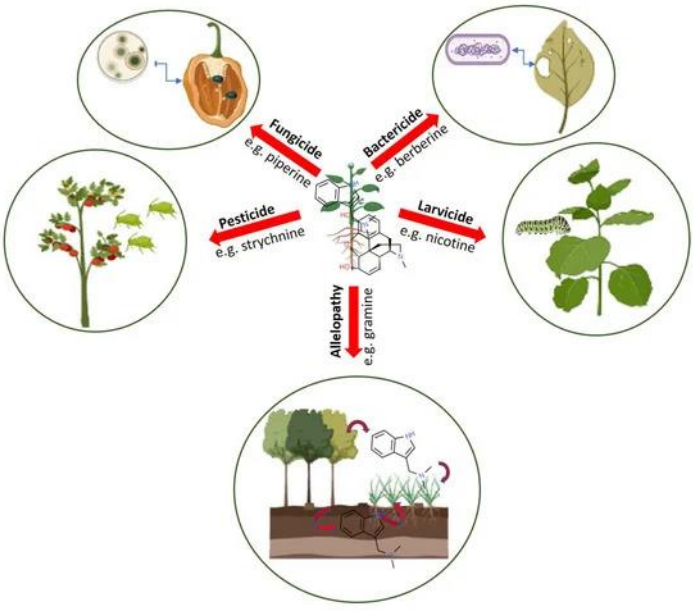

The specialised alkaloids are stored in various cellular parts, upon sensing different environmental stress conditions (6). When the plant is exposed to a stress condition, the alkaloids are released from the stored organelle and exported to the target tissue (7). They are used to fight

against various predators (such as pests, fungi, bacteria and larvae) and provide the plant protection by acting like a chemical barrier and causing harmful effects in predators (***Figure 1.1***). Another function of the alkaloids is, that they can also stop the growth of other plants in the vicinity (allelopathy) (1). Plants growing on high nitrogen soils and nitrogen-fixing plants, accumulate high levels of alkaloids, making them more resistant.

Figure 1.1 **(1)**
Overview of the function of alkaloids in plant defence. Alkaloids are produced in various cell tissues and provide plant protection against predators.

1.1.3. Human alkaloid exposure

Accidental alkaloid exposure occurs mainly through contaminated cereals, pseudo-cereals, legumes, grains, herbal teas and spices (8). These food products are a major part of the diet for all age groups in the world population. The screening of these products is a major health concern (9). Pseudo-cereals (such as buckwheat, chickpea, quinoa) gained a great popularity and commercial interest in the last years. These products have a lot of healthy properties like being rich in vitamins, proteins and the absence of gluten (8). Besides the advantages, alkaloids are often present in these products so careful controlling systems are necessary. The most common contamination route is related to the co-harvesting of weeds, which share the same cultural cycle. The risk is theoretically higher for seed-bearing plants which are mechanically harvested (10). During processing, leaves from vegetables can be mixed with leaves from toxic alkaloid-producing plants.

Alkaloids are very heat resistant, boiling water may not be able to effectively reduce the toxic compounds (5). Animals can also be exposed to plant toxins mainly through contaminated feed or alkaloids that end up in the river and are consumed. Poisoning through the consumption of animal-derived products is unlikely but there is a need for more research (8). Recently, the biological activities of different plant tissues have been extensively studied (4).

Berberidaceae, Amaryllidaceae, Papaveraceae, and Solanaceae, belonging to the higher plant species, are prominently richer in alkaloids (1). Furthermore, across different plant families, different classes of alkaloids are found. This depends on the biosynthetic pathway in a particular species. Thanks to the detailed study of secondary metabolites through chemical approaches, there is now a comprehensive understanding of the diversity in the alkaloids (11).

1.1.4. Toxic effects of alkaloids

Traditionally, plant extracts have always been used as medicines all over the world. Since the nineteenth century, bioactive compounds have been used for the production of psychoactive and therapeutic drugs. Different molecular structures within the alkaloid classes express different toxicological effects (1).

The anticholinergic compounds atropine and scopolamine (tropane alkaloids) are one of the most important medicinal alkaloids. They have been useful in treating multiple pathologies and symptoms such as nausea, vomiting, heart or respiratory problems, as an antispasmodic in gastrointestinal problems, anti-allergic drugs, and even as an pupil dilator for ophthalmic treatment (12). Despite their great medicinal advantages, tropane alkaloids have been implicated in numerous intoxications. The anticholinergic activity avoids the binding of acetylcholine with the muscarine receptor (13). These toxic effects cause tachycardia, muscle spasms, mydriasis, delirium and can sometimes even cause death (14).

Pyrrolizidine alkaloids (PAs) are considered the most widely distributed natural toxins. Exposure to contaminated grains or plants can result in three main effects: hepatotoxicity, mutagenicity and carcinogenicity (3). The intoxication can result in acute, sub-acute and chronic effects. Haemorrhagic necrosis, hepatomegaly and ascites are considered as acute effects. Sub-acute, there is a blockage of the hepatic veins. Chronic PA exposure, results in fibrosis and cirrhosis of the liver. The highest level of toxicity results in liver failure and eventually death (15). The penetration of the PAs in the nucleus, is the main mechanism of toxicity and cause DNA cross-links and DNA-protein cross-links. This disrupts the normal functioning of the cell and cause damage. The bioactivation of the compounds occurs mostly in the liver, therefore the

hepatocytes are the main target of toxicity (15). This DNA damage can be the base of development for different types of cancer. Veno-occlusive disease (VOD), is the most common clinical manifestation. The symptoms include, bleeding diarrhoea, vomiting and liver enlargement (9).

In many countries opium seeds are a popular to make tea. These seeds do not contain opium itself but contamination can be caused by insect damage or poor harvesting. For children and vulnerable people, consumption can involve many risks. Due to opium contamination, false positive drug tests and intoxications have been reported (16). Ergot alkaloids are another class of toxic secondary metabolites, which induce their toxicity by the interaction with neurotransmitters (17). Necrose and apoptosis in human kidney cells are the most commonly reported effects of a high exposure. The ergot alkaloids cause complex effects on cardiovascular function and increase the uterine motility (9). Because of the high toxic potential of alkaloids, the reduction of undesirable toxic compounds must be ensured by the food manufacturing companies.

1.1.5. Regulatory evolution of alkaloid exposure

The Scientific Panel on Contaminants in the Food Chain (CONTAM) is part of the European Food Safety Authority (EFSA) and is responsible for public health related to food and feed. On 8 November 2011, the first scientific opinion was published by the authority about the presence of PAs in different food matrixes (18). The panel decided to apply the Margin of Exposure (MOE) approach instead of a Tolerable Daily Intake (TDI). A Benchmark dose lower confidence limit ($BMDL_{10}$) to excess cancer risk of 70 µg/kg body weight (bw) per day was calculated for lasiocarpine exposure in male rats. This value was used as reference point (RF) for comparison with the estimated dietary exposure. $BMDL_{10}$ is the 95 % lower confidence limit of the benchmark dose (minimum dose that produces a clear, low level health risk) (19).

In April 2013, a proposal was published by the Authority to investigate PA levels in different types of animal and plant-derived food products. Different products like eggs, milk products, meat products, herbal teas and food supplements were

investigated. On the third of August 2015 the outcome of this study was published by the authority (11). One or more PAs were detected in 60% of the food supplements, 2% of the animal derived products and in 91% of the herbal tea samples. Striking, all the investigated teas were found to contain PAs, with a mean concentration of 6.13 µg/L in tea infusion.

The authority published on 26 August 2016 a new scientific report about the dietary PA exposure in the European population (20,21). It was concluded that herbal teas and infusions were by far the main contributors to human exposure to PAs. Pollen-based supplements and honey, were second in row. Because of these results, the CONTAM Panel established in July 2017 a reference point of 237µg/kg body weight per day (22). The RP was derived from the incidence of liver sarcoma in female rats, exposed to riddelliine. To monitor the presence of alkaloids in plant-based food, the panel recommended the development of more sensitive and specific analytical methods.

On 11 December 2020, the European Commission published the newest update of the Regulation on maximum levels of PAs in certain foodstuffs (23). This regulation is binding and directly applicable to all the European Member States. The maximum levels (µg/kg) refer to the sum of 35 EU-Regulated PAs. This law is enforced from 1ste July 2022 set in EC Reg. (EU) 2020/20405. The alkaloids were determined in different types of products and are listed in the table below (***Table 1.2***).

Table 1.2 **(23)**

Regulation on the maximum levels of PAs in certain foodstuff. "**" means that the maximum level refers to the "lower bound sum" of the following 21 Pyrrolizidine alkaloids: intermedine/lycopsamine, intermedine-N-oxide/lycopsamine-N-oxide, senecionine/senecivernine, senecionine-N-oxide/senecivernine-N-oxide, seneciphylline, seneciphylline-N-oxide, retrorsine, retrorsine-N-oxide, echimidine, echimidine-N-oxide, lasiocarpine, lasiocarpine-N-oxide, senkirkine, europine, europine-N-oxide, heliotrine and heliotrine-N-oxide.

	"Foodstuffs (1)	Maximum level (*) (µg/kg)
8.4.	**Pyrrolizidine alkaloids**	
8.4.1.	Herbal infusions (dried product) (**) (***) with the exception of the herbal infusions referred to in 8.4.2. and 8.4.4.	200
8.4.2.	Herbal infusions of rooibos, anise (*Pimpinella anisum*), lemon balm, chamomile, thyme, peppermint, lemon verbena (dried product) and mixtures exclusively composed of these dried herbs (**) (***) with the exception of the herbal infusions referred to in 8.4.4.	400
8.4.3.	Tea (*Camellia sinensis*) and flavoured tea (****)(*Camellia sinensis*) (dried product) (***) with the exception of the tea and flavoured tea referred to in 8.4.4.	150
8.4.4.	Tea (*Camellia sinensis*), flavoured tea (****)(*Camellia sinensis*) and herbal infusions for infants and young children (dried product)	75
8.4.5.	Tea (*Camellia sinensis*), flavoured tea (****)(*Camellia sinensis*) and herbal infusions for infants and young children (liquid)	1,0
8.4.6.	Food supplements containing herbal ingredients including extracts (**) with the exception of the food supplements referred to in 8.4.7.	400
8.4.7.	Pollen based food supplements (19) Pollen and pollen products	500
8.4.8.	Borage leaves (fresh, frozen) placed on the market for the final consumer (**)	750
8.4.9.	Dried herbs with the exception of the dried herbs referred to in 8.4.10. (**)	400
8.4.10.	Borage, lovage, marjoram and oregano (dried) and mixtures exclusively composed of these dried herbs (**)	1 000
8.4.11.	Cumin seeds (seed spice)	400

1.1.6. Classification of plant alkaloids

Plant alkaloids have a wide range of biological properties, achieved by various functional groups attached to the central moiety (1). The arrangement and combination of functional groups is providing a diverse range of alkaloids (***Figure 1.3***). Within a particular genus of plants, many alkaloids share a common skeleton nevertheless they differ in their biological and chemical properties (1). The biological diversity of alkaloids is catalysed by chemical reactions like

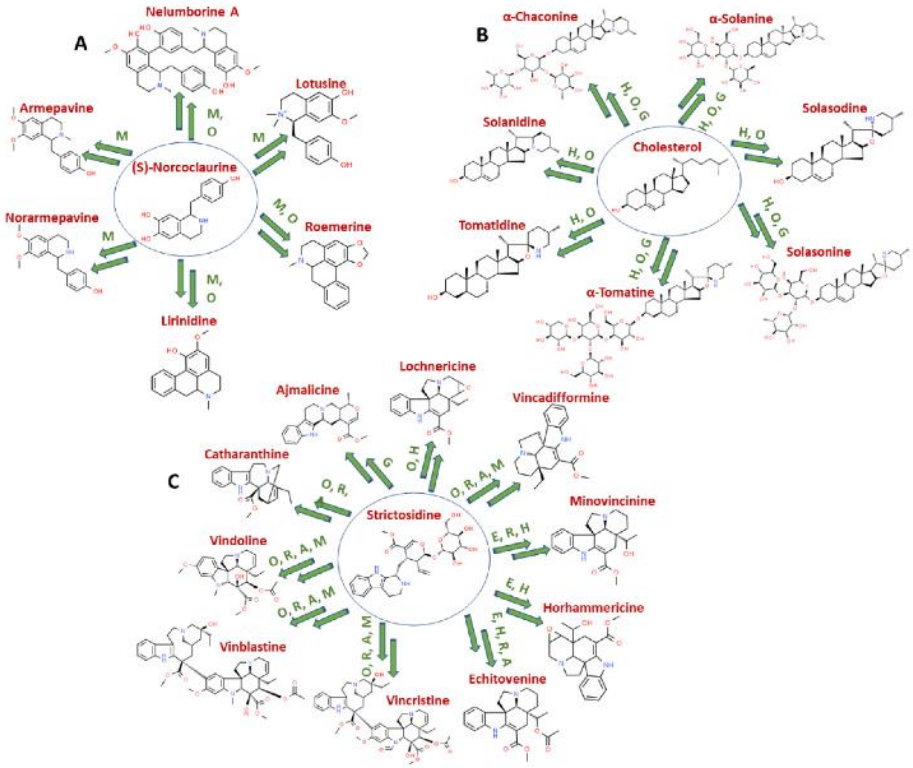

methylation, glycosylation, oxidation, reduction, hydroxylation and acylation. The structural modifications generate a broad range of specialised secondary metabolites.

Figure 1.3 **(1)**
Multiple alkaloids in different plant species are biosynthesised from these same skeleton. The basic structure of the central moiety is represented in the blue circles. (A) Benzylisoquinoline alkaloids (B) Steroidal alkaloids (C) Terpene indole alkaloids The arrows represent the key enzymatic conversions that the common skeleton undergoes. (R = reduction, A = acetylation, E = epoxidation, M = methylation, H = hydroxylation, O = oxidation, G = glycosylation)

The plant alkaloids are further classified into 3 big groups according to different plant characteristics; 1) chemical structure 2) biosynthesis pathway 3) taxonomical groups (24). When the alkaloids are classified by their chemical structure, they can be grouped under heterocyclic and non-heterocyclic compounds. This is based on the position of the nitrogen atom within the chemical skeleton. Alkaloids formed by the decarboxylation process of amino acid precursors like (L-tyrosine, L-phenylalanine, L-ornithine, L-tryptophan, L-lysine, and L-histidine) are heterocyclic, when nitrogen is present in the main ring. On the other hand, when the nitrogen atom is present in the aliphatic chain and occupies another position than in the heterocyclic ring, non-heterocyclic alkaloids are formed.

Alkaloids can be grouped by being biosynthesized from a similar biochemical precursor (25). For example, amino acid precursors like tyrosine, tryptophan and lysine respectively become indole, pyrrolizidine, and piperidine alkaloids by enzymatically catalysed chemical reactions. Anthranilic acid is a non-amino acid precursor which gives rise to Quinoline alkaloids by supplying a nitrogen atom.

The third way to classify Alkaloids is by taxonomy, this leads to expanded knowledge regarding the distribution of specialised metabolites in different plant species. This means that alkaloids derived from the same genera of plant species are classified under one category. For instance, morphine, codeine, noscapine, thebaine, and papaverine, are all produced in the same species *Papaver somniferum L*. and grouped under opium alkaloids (24).

1.2. PYRROLIZIDINE ALKALOIDS

1.2.1. General introduction

Pyrrolizidine alkaloids (PAs) are considered the most distributed natural toxins. These toxic compounds are found in plants from different taxa, all over the world (3). Some PAs can also be found in insects, which take up the alkaloids and use their properties as a benefit to fight predators (15). Toxicity is mostly occurring due to the use of PA contaminated grains or plant species for herbal teas and traditional medicine.

The human PA exposure frequently exceeds the maximum daily intake suggested by authorities. Exposure is in most cases insufficient to cause poisoning, but can be a contributory factor to chronic diseases like cancer (15). The PA alkaloids are derived from ornithine and include a wide range of structural diversity. The common skeleton of PAs is composed of one or more necic acids (mono- or dicarboxylic aliphatic acids) and a necine base (amino alcohol), structurally they are mono or diesters.

The chemical structure can either occur as a tertiary base or as their corresponding N-oxide (PANO) (26). The pyrrolizidine core is composed of two five-membered rings. The rings can occur in a saturated and an unsaturated form, and are connected by a nitrogen atom (27). The unsaturated form has a double binding in the 1,2 position, this results in an enhanced toxicity (***Figure 1.5***). Although the 1,2 unsaturated forms all have a common structure, they differ in potency and express different symptoms. The toxicity level is the highest for cyclic diesters, non-cyclic diesters are medium toxic and monoesters express the lowest toxicity (28). The effects are associated with acute toxicity, which could result in genotoxicity, hepatoxicity, carcinogenicity and liver damage (19).

In contrast, PAs without the 1,2 double bound show lower toxic effects. To exert their toxic effects, the statured forms must be metabolised. Metabolization occurs by enzymes present in hepatocytes whereafter waste products are excreted through the urine (26) (29). These enzymes are expressed at very low levels, therefore saturated

necine bases are considered as non-toxic and not taken into account for the quantification. Otherwise, the health risk caused by the intake of pyrrolizidine alkaloids would be overestimated.

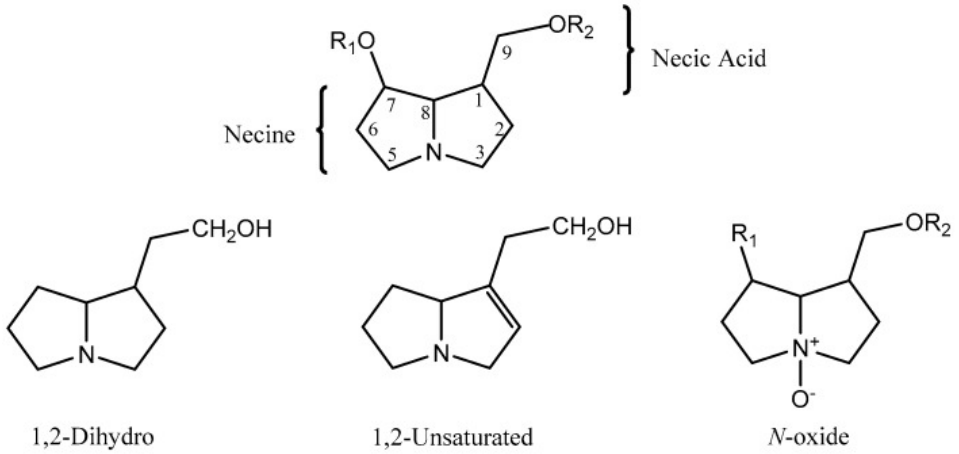

***Figure 1.5* (15,30)**
Overview of the pyrrolizidine alkaloids skeleton in its different forms.

1.2.2. Occurrence of Pyrrolizidine alkaloids in herbal teas

For decades plant-derived products are worldwide consumed for a variety of medicinal and culinary use (8). They are frequently used as natural additives to extend shelf-life and improve sensory properties. Some condiments are also used as ingredients to prepare infusions. Herbs and spices have a risk to be accidentally contaminated (31). These toxins are relatively heat-stable, that is why herbal infusions and teas which are positive for alkaloids, can cause major problems. The occurrence of PAs in commercially available teas has gained increasing attention from the EU.

Samples of chamomile, peppermint and rooibos tea, contain generally the highest PA levels. The amounts in black and green tea are typically lower (32). Especially the cyclic diesters and open-chain diesters like for example lasiocarpine and senecionine, have the highest potency factor. On average, the main contributors to the total PA concentration are*:* intermedine, intermedine-N-oxide, lycopsamine, senecionine, senecionine-N-oxide, seneciphylline, seneciphylline-N-oxide and retrorsine-N-oxide (32). According to the EFSA rapport from 2017, these eight PAs represented 95% of the total PA concentration in black tea, 90% in chamomile, 92% in rooibos, 78% in green tea and 83% in peppermint (32).

1.3. CHROMATOGRAPHIC TECHNIQUES

1.3.1. General overview

Chromatography is a widespread physical separation and purification method. A mixture is separated in its components based on their physicochemical properties. To enable the separation, a stationary and mobile phases are essential. The column is packed with an immobile and porous stationary phase (33,34). The mobile phase can occur either as a liquid or gas, this makes the difference between liquid or gas chromatography. The separation is based on the principle that every component will exhibit a different affinity for the stationary phase. The molecules will migrate with the mobile phase through the column (35,36).

The equilibria between the two phases, results in components eluting on other moments from the column. A detector at the end of the column will record a chromatogram that displays the signal as a function of time. Resolution (RS) is an essential parameter for good separation. Each peak should be symmetrical and should only contain one component. Size and length of the column, type of eluent and temperature are some variables that can be adjusted to improve the resolution (37).

1.3.2. Reversed-phase high pressure liquid chromatography

In this master thesis, the reversed-phase high pressure liquid chromatography (RP-HPLC) separation technique is used. This technique uses a hydrophobic stationary phase and a hydrophilic mobile phase. As mentioned above, separation is based on the physiochemical properties of the molecules (38,39). The compounds with hydrophobic properties will show more interaction with the stationary phase and are retained longer on the column (40). An RP-HPLC device contains the following components; 1) solvent delivery system, 2) a pump, 3) an injector, 4) a column for separation, 5) a detector and a collection device.

The solvent delivery system is responsible to compose the desired gradient. This gradient is delivered to the column with high pressure because of a pump (41). The pump provides a constant speed, when the mobile phase is moving through the column (42). The injector ensures a quick and direct injection of the sample into the

mobile phase. Consequently, the mobile phase passes through the column where the separation occurs, based on polarity (40). The separation can be improved by adjusting some parameters of the column like temperature and length (42). Hereafter, the compounds elute from the column and reach the detector. The detector measures the substance of interest based on its physical properties. Finally, the data is converted into a visual representation by the collection device (41).

1.4. MASS SPECTROMETRY

1.4.1. General overview

Mass spectrometry (MS) is an analytical technique consisting of three essential components: an ion source, an analyzer and a detector. It has become a routine technique over the last years. A large part of the success is due to its ability to give three-dimensional data (43). MS is often coupled with an HPLC or Ultra-performance liquid chromatography (UPLC) device to separate different components in time. Both methods are liquid chromatography techniques, however UPLC performs at higher pressures and allows lower particle size in the column. The ionization source generates ions, which are then separated by the mass analyzer according to their mass-to-charge ratios *(m/z)* (44). Thereafter the abundance of each ion is measured by the MS detector (45). MS can be used for analyzing more complex samples. Even at low levels in complicated matrices, compounds can be successfully determined.

1.4.2. Ion source

Only gaseous and ionised molecules can be analysed by a mass spectrometer. Therefore, the ionisation source is an essential component of the MS device. The ionisation source will convert the molecules into the gas phase and perform ionisation. Electron spray ionisation (ESI) and Matrix-assisted laser desorption ionisation (MALDI) are the two most common used systems (46,47). In this master scription ESI is used, which converts molecules in the liquid phase into gaseous ions. The transition to gas phase ions occurs in three steps (48).

The sample is first injected into a stainless-steel tube (needle) which is exposed to a nebuliser gas and a voltage ranging from 3 to 5 V. This will create a homogeneous flow of droplets and formation of a spray in the tip of the needle due to a high voltage. In this spray, a mixture of droplets with different charges is present. The droplets will feel the electric field between the inlet of the first analyser and the needle (48). Therefore they are attracted towards the analyser inlet.

Second, because of the presence of an organic solvent and the heat of the needle, the medium will start to evaporate. This happens as soon as the droplets are released from the needle (47). Thirdly, the phenomenon of ion expulsion occurs. The surface tension is overcome by the repulsion, which makes it energetically possible for ions to enter the gas phase. Once in the gas phase, the molecules can pass into the analyser. One of the advantages of this method, is the possibility to make a direct an automated coupling with HPLC (49).

1.4.3. Analyser

The analyser will analyse the ionised molecules in the gas phase. The quadrupole (Q) and the time of flight analyser (TOF) are the most frequently used (50). The TOF-tube principle is as follows: ions acquire a certain speed because they are accelerated by an electric field at the beginning of the tube. Subsequently, they enter a field-free tube of a certain length (51). The molecules with a greater mass will need a longer time interval to travel to the specific distance in the tube. For this reason, lighter molecules will arrive first at the detector.

The fact that the tube is sensitive to temperature fluctuations, can be a problem (52). The measurements are affected by these in changes tube length. The tube will expand at higher temperatures and will shrink when it is exposed to lower temperatures. For this reason, regular calibrations are a must to know the exact length of the tube. The major advantage of the TOF analyser is its close mass accuracy and its high sensitivity (53). The second analyser is a Q, which is composed of four round bars. These bars are placed symmetrically on the opposite side of each other. When the ions reach the Q analyser, they will be oscillating between the bars because of the applied radiofrequency (RF) and voltage. Only ions with a determined speed and

specific predefined *m/z* ratio, will be let trough. The RF and voltage are changed all the time, to filter very specific for the desired *m/z* ratio (47,51,52).

1.4.4. Detector

After the right ions are selected, the detector measures their presence (54). The most common detector is an electron multiplier (EM). An amplifier will boost the current, which is created by the ions. Otherwise, this current would be too weak to create a proper signal. The amplifier consists of a series of dynodes, which will attract the ions due to an electric field (55). In this series of dynodes, every successive dynode contains a higher voltage. The ions are colliding against the dynode, and will fall apart in secondary electrons. As a result, an electron cascade is initiated which results in an amplification of the start signal. Via a simple back calculation, the original start signal of the ions can be calculated (54,56).

1.4.5. Tandem mass spectrometry (MS/MS)

After the compounds leave the RP-HPLC, the alkaloids will be identified and quantified using tandem mass spectrometry (MS/MS). This technique connects two analysers in series (tandem), separated by a collision cell. When the ions enter the analyser, they will be separated based on their *m/z* ratio (51). Successively, ions are fragmented when entering the collision cell. Thereafter, the ions enter the second analyser and are separated for the second time based on their *m/z* values (52). Finally a mass spectrum is formed when the ions are detected (***Figure 1.6***). MS/MS is different from other techniques because the fragment ions add an additional level of information. In this way, the identification of precursor ions with similar *m/z* values is facilitated (57).

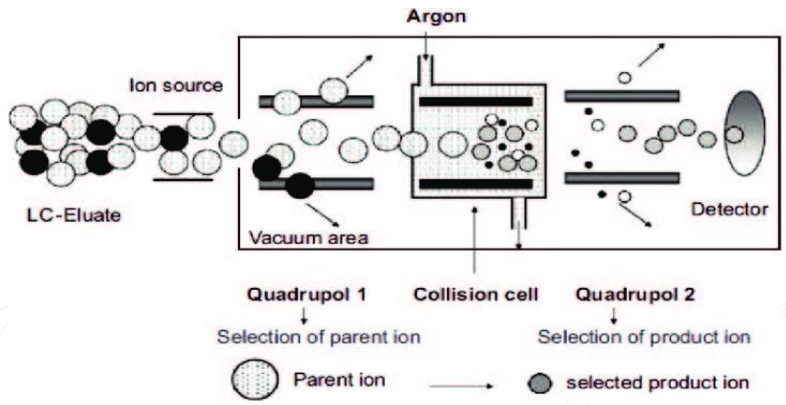

***Figure 1.6* (58)**

General principle of tandem mass spectrometry (MS/MS). Firstly, the compounds are ionised and separated based on their m/z values by the quadrupole. Thereafter the collision cell fragmentates the precursor ion. Finally, the second analyser separates the fragments, whereafter they will be detected by a detector.

1.5. VION IMS QTOF MASS SPECTROMETRY

Ion mobility mass spectrometry (IM-MS) is a powerful technique to screen both targeted and non-targeted compounds. The technique distinguished itself from other techniques by its ability to separate isomeric and isobaric compounds, minimize back ground noise and reducing the false negative detections (59). This technique found great utility for biomolecular separation. Nevertheless, this approach remains unexplored in food safety. Creating collision cross-section (CCS) data bases is required to implement IM-MS in pyrrolizidine alkaloid workflows, to serve as an additional molecular identifier (60).

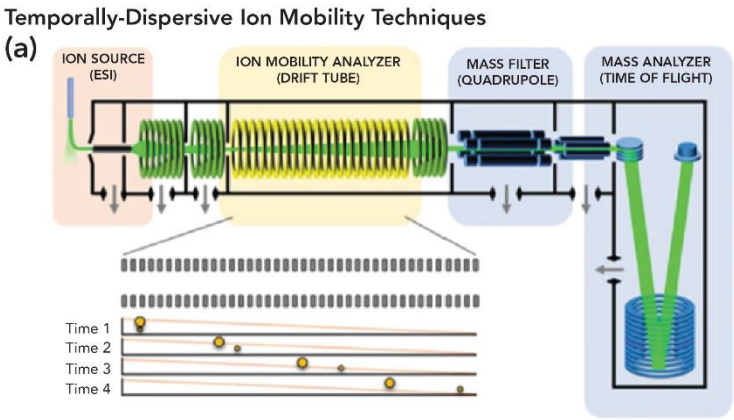

***Figure 1.7* (61)**

Conceptual diagram of IM-MS instrumentation. An ion mobility spectrometer electrostatic drift tube, coupled to a quadrupole time-of-flight (QTOF) mass spectrometer.

1.5.1. Ion mobility mass spectrometry (IM-MS)

Ion mobility spectrometry (IMS) is a separation technique, which combines size and mass-selective separations into a single analytical technique. Generated ions are separated based on their mobility. This occurs in a carrier buffer gas which flows through the drift tube under atmospheric pressure and an electric field. (***Figure 1.7***) provides a conceptual schematic overview of the technique. The mobility (drift time) of an ion depends on its charge, size and shape. Differences in these molecular conditions, lead to differences ion movement in the drift tube and allow their separation (62).The drift times are instrument and application specific, therefore the parameter is not practical to use. To allow instrument

comparison, reporting of a collision cross-section parameter is preferred (59). CCS values can be calculated by applying the the Mason-Schamp equation or can be predicted by machine learning algorithms (61).

1.5.2. Collision cross section (CCS)

CCS is an orthogonal molecular identifier, independent from the complexity and concentration of the matrix. CCS offers the opportunity to further improve the identification process, based on unique physiochemical properties of a molecule (60). Unlike conventional mass spectrometry using *m/z* ratio's, components are separated based on their specific chemical structure (63).

1.6. VALIDATION PROCEDURE

Validation is a necessary process, which establish scientific evidence that the developed method is capable to deliver qualitative results in a consistent way. To perform a scientifically correct validation, a fixed structure of test must be performed according to guidelines. (***Figure 1.8***) in attachments gives an overview of a possible sequence of operations in LC-MS/MS method validation (64).

A first part of the validation, is to select a calibration graph approach. Either a calibration graph in solvent or a matrix-matched calibration can be performed. The advantage of this last approach is the compensation for recovery loss and ionisation suppression/enhancement (64). The term linearity is defined as the ability to obtain results which are directly proportional to the analyte concentration. Trueness, accuracy and precision are related to the agreement between a reference value and the measured value. Recoveries are calculated to asses whenever the method is adequate or not. The recovery of a method is calculated by taking the ratio from the peak areas before and after spiking (44,65). Co-eluting compounds (late eluting compounds from previous samples or matrix compounds from the sample) can strongly influence the ionisation process. The term matrix effect includes both the ionisation suppression and enhancement of the analyte. It is the combined influence of all components other than the analyte on the LC-MS ionisation process (44)(65).

2. OBJECTIVE

To get a first idea about the incidence of pyrrolizidine alkaloids (PAs) in commercially available tea, 15 matrices were screened, using A Vion IMS QTOF Mass Spectrometer. The analytical method was already operatable, however a new extraction protocol was elaborated from scratch, to simplify the process. Different extraction methods were compared to selected the most optimal approach. Too few samples were analysed to draw a statistical conclusion for the whole market. These screening test, were mainly performed to get an initial idea about the contamination problem, and to get the opportunity to work with a TOF analyser. Thereafter, the contamination results were matched with literature findings.

Pyrrolizidine analysis remains a challenge seen their structural similarities, the lack of analytical standards and the presence of isomeric forms. To overcome these analytical challenges, an ion mobility-derived collision cross-section database could provide a solution. The implementation of Ion mobility (IM) within the food analytical field is quite new. Very few contaminant databases are already disposable. The aim was, to provide the first available alkaloid library, containing the 35-Eu regulated PAs. Theoretical predictions were obtained by two algorithms, trained by a machine learning approach (*AllCCS* and *CCSbase*). As a proof of concept, the created database was correlated with experimental CCS values, by calculating a prediction error.

Seen the latest information on serious genotoxic and carcinogenic properties of PAs, there is a need of more efficient and specific analytical methods. The available TOF method described above, was rather suitable for screening than quantification. Quadrupole analyzers are more accessible and favored to perform quantification. Because of the high cost and limited availability of TOF analysers, there was a need to transfer this screening approach to a less expensive and user-friendly triple quadrupole (QqQ) protocol. The aim of this work was, to contribute to the first stages of development of a new UPLC-MS/MS method, using a QqQ analyser. This technique must be able to simultaneously determine and quantify 21 PAs in commercially available tea samples. The available TOF protocol was used as a starting point for the first developmental stages of the new QqQ method. This way, the laboratory of

professor Dall'Asta could perform simple routine quantification of different types of teas. In a later stage, after optimalisation and validation, the developed method could be used in food manufacturing companies to prevent contaminated tea to enter the market.

A standard mixture containing 21 PAs was used, to search for the ideal UPLC-MS/MS conditions, which could separate and identify the components in the mixture. During different runs, the most optimal gradient, mobile phases, injection volume, collision energy, and flow rate, were searched to analyse PAs in tea. This method only included 21 of the 35 PAs listed by the European Regulation (23). The 21 Pyrrolizidine alkaloids which the method will try to separate and detect are*: intermedine, lycopsamine, intermedine-N-oxide, lycopsamine-N-oxide, senecionine, senecivernine, senecionine-N-oxide, senecivernine-N-oxide, seneciphylline, seneciphylline-N-oxide, retrorsine, retrorsine-N-oxide, echimidine, echimidine-N-oxide, lasiocarpine, lasiocarpine-N-oxide, senkirkine, europine, europine-N-oxide, heliotrine and heliotrine-N-oxide.* The molecular structures can be found in (***Figure 2.1***) in attachments.

3. MATERIAL AND METODS

Table 3.1

Overview of used products and devices with corresponding manufacturer.

Products	Manufacturer
Ammonium formate	Sigma-Aldrich (Missouri, US)
Formic acid	Carlo Erba Reagents (Emmendingen, Germany)
Methanol	VWR Chemicals (Pennsylvania, US)
Water	VWR Chemicals (Pennsylvania, US)
Devices	**Model/ Manufacturer**
Centrifuge	Eppendorf centrifuge 5810R (Leipzig, Germany)
Shaker	IKA- Werke HS501 Digital (Staufen, Germany)
Analytical balance	Ohaus PA214C (Missouri, US)
Ultrasonic cleaner	VWR (Pennsylvania, US)

3.1. SAMPLE ANALYSIS WITH AN IMS TOF ANALYSER

15 commercially available tea matrices were screened for PA contamination. The samples were analyzed in duplicate by an ion mobility mass spectrometry (IM-MS) time of flight (TOF) method, available in the laboratory. The TOF method screened for the 35-EU regulated PAs, and follows the protocol described in article (66). However, a new liquid-liquid extraction (LLE) method was searched in literature to simplify the extraction process. Product information of the 15 analyzed samples can be found in (***Table 3.2***) in attachments.

3.1.1. Extraction method

The 15 samples were analyzed in duplicate and submitted to the following extraction procedure. 5 tea bags of each tea box were combined and shaken in order to become a representative sampling. 1 g of each sample was weighed and submitted to the extraction procedure. The tea sample (1.00 g) was put into a 50-mL centrifuge tube. The extraction solvent (methanol: water: formic acid, 60:39.6:0.4, v/v/v) was made. 10 mL of the extraction solvent was added to the centrifuge tube. The suspension was shaken (240 min^{-1}, 30 min,) and centrifuged (13.081 g, 5 min, 4°C). The supernatant was micro-filtered (0.22 µm) and captured in an amber-glass vial (2-

mL). Only high purity solvents were used in the TOF analyzer. Different possible LLE methods were collected form literature and are displayed in (***Table 3.3***) in attachments.

3.1.2. Applied liquid chromatography conditions

The chromatographic analysis were performed, using an ACQUITY™ UPLC I-Class PLUS System with column manager. The autosampler was a flow Through Needle injector (FTN) with 15 µL needle. For the column an ACQUITY UPLC BEH™ C8 (2.1 × 100 mm, 1.7 µm particle size, 130 Å pore size, p/n: 186002878, *Waters Wilmslow, UK)* was used. The needle wash solvent contained; Water: methanol: acetonitrile: isopropanol (20:40:20:20 + 0.5% formic acid volumetrically). The seal wash solvent was composed of water: methanol (80:20, v/v%). The temperature of the column and sample were respectively 40°C and 10°C (66).

The aqueous phase contained 5 mM ammonium formate in water + 0.1% formic acid (v/v). The organic phase was composed of acetonitrile + 0.1% formic acid (v/v). The flowrate was set at 0.3 ml/min and an injection volume of 5 µL was applied. The following gradient program was used to achieve separation of target compounds. Starting at 95% mobile phase A (MPA) at time 0, MPA decreased to 85% in 12 min. At 20 min, MPA was set at 65% and thereafter it decreased drastically to 5% in 0.5 min. These conditions were maintained until 22 min. Subsequently, the initial conditions were restored at 22.1 min and the column was re-equilibred for 2.4 min. The total runtime was 24.5 minutes. (***Table 3.4***) in attachments gives an overview of the applied gradient.

3.1.3. Applied mass spectrometry conditions

The PAs and their corresponding PANOs were detected by an ACQUITY UPLC separation system coupled to a traveling wave ion mobility mass spectrometer (*Waters Corporation, Manchester, UK*). The mass spectrometry detection was conducted in positive electrospray ionization (ESI) mode, in the mass range of *m/z* 100-1000. The instrument parameters were listed as follows: the capillary voltage was operated at 0.75 kV in positive mode; the cone gas flow was set at 50 L/Hr. A desolvation

temperature of 600°C, a desolvation gas flow of 850 L/Hr and source temperature of 150°C, were applied. The TOF analyser was operated in sensitivity mode. Regarding IMS conditions, the following settings were applied. The nitrogen flow rate was set at 90 mL/min (3.2 mbar; wave velocity, 650 m/s) and a wave height of 40V. Data acquisition was conducted using UNIFI 1.8 software *(Waters, Wilmslow, UK).*

3.2. ION MOBILITY-DERIVED COLLISION CROSS-SECTION DATABASE

Two different algorithms trained by machine learning, were used to predict theoretical collision cross-section (CCS) values for each PA. The software employs a training dataset, through which the machine-learning algorithm, is able to predict CCS values for novel structures. *AllCCS* (http://allccs.zhulab.cn/) and the more recently developed *CCSbase* (https://ccsbase.net/) were the applied predictive tools. The simplified molecular-input line-entry (SMILE) of the 35-Eu regulated PAs were imported in the “prediction section” of both online interfaces. The CCS values were provided by the algorithms, for the following ions; $[M+H]^+$, $[M+H-H2O]^+$, $[M+Na]^+$, $[M+NH4]^+$, $[M-H]^-$, $[M+Na-2H]^-$, $[M+HCOO]^-$. This information was combined into the first available CCS database for the 35 EU-regulated PAs.

To obtain the experimental CCS values, a standard of the targeted PAs was injected into the Vion, in two different dilutions (200 and 20). Thereafter, the device was commanded to calculate the mean observative CCS for every alkaloid. The observed CCS values, were only displayed for the most abundant ion $[M+H]^+$. Thereafter, the experimentally obtained and theoretical CCS values were compared, by calculation of a prediction error.

3.3. TRANSFERING THE TOF METHOD TO A QUANTIFYING QqQ METHOD

There was a need to transfer the available IMS TOF screening method to a user-friendly triple quadrupole (QqQ). This new method will be used for analysis and quantification of PAs in tea. The protocol described above was used as a starting point

for the development of the new UPLC-MS/MS protocol (66). A standard mixture containing 21 pyrrolizidine alkaloids was available in the lab. A concentration of 100 ppb of the mixture was injected, to search for the most optimal UPLC-MS/MS parameters. Different runs were performed in order to select the conditions that could separate and identify the different PAs in the mixture and give clear fragments. Multiple options of different mobile phases, gradients, flow rates and collision energies, were tested. The column was first washed with pure MeOH to make sure no compounds from previous runs were left on the column.

3.3.1. Liquid - chromatography conditions

The chromatographic analysis was similar to the TOF protocol, described above. The same conditions were used for the chromatographic system, autosampler, injector, column, needle wash solvent, seal wash solvent, column temperature and sample temperature. The aqueous and organic mobile phase differ from the TOF protocol. Water (phase A) and methanol (phase B), both in addition of 2 mM ammonium formate in water + 0.2% formic acid (v/v%), were used. To obtain these solvents, 2 mL formic acid and 0.126 g ammonium formate were added to 1 L of both phases. The organic phase was placed in the ultrasonic cleaner to help ammonium formate dissolve and reduce the air bubbles. Ammonium formate dissolved better in the aqueous phase, ultrasonic cleaning, was not necessary. The flowrate was set at 0.3 ml/min and an injection volume was corrected to 3 µL. An overview of the applied liquid-chromatography conditions of the new QqQ method, can be found in (**Table 3.5**) in attachments.

The following gradient program was optimized to achieve separation of target compounds. Starting at 100% mobile phase A (MPA) at time 0, MPA decreased to 90% in 1 min, these conditions were held for 1 min. At 6 min, MPA was set at 80% and thereafter it decreased to 60% in 1 min. MPA was 50% at 13 min and 40% at 15 min. A drastic drop to 0% in 1 min, whereafter this conditions were held until 18 min. Subsequently, the initial conditions were restored in 1 min and the column was re-equilibrated for 6 min. The total runtime was 25 minutes. (***Table 3.6***) in attachments displays the applied gradient.

3.3.2. Mass spectrometry conditions

Most of the mass spectrometry conditions were similar to the ones applied in the TOF protocol. The ionization mode, acquisition mode, capillary voltage, cone gas flow, desolvation temperature and software, remained similar to the method described above. (**Table 3.7**) in attachments displays the applied mass spectrometry conditions, of the new developed QqQ method. The collision energies (CE) were optimised to get an improved ion intensity. Specific collision energies were chosen, based literature review. An overview of the specific applied collision energies can be found in (***Table 3.8***).

4. RESULTS

4.1. SAMPLE SCREENING USING IMS QTOF MASS SPECTROMETRY

4.1.1. Extraction method

All of the samples were submitted to the extraction procedure described above. The liquid-liquid extraction (LLE) protocol was based on following article (8). A low centrifugation temperature, to help precipitate the solid parts, was added to this method. After centrifugation and filtration, clear extraction products were obtained for all of the samples. Solid-liquid extraction (SLE), is often applied in literature, to eliminate a part of the matrix co-extractives. Seen the chemical complexity, it was not applied to the tea matrices, because the goal was to simplify the extraction protocol. (***Table 4.1***) in attachments gives an overview of possible SLE methods with additional clean-up, collected from different literature sources.

4.1.2. Samples analysis

After screening, using the IMS TOF method described above, 14 of the 15 analysed tea samples were contaminated. The contaminating PAs in each sample, are displayed in (***Table 4.2***). The tea samples were screened for the 35-Eu regulated PAs. A combination of multiple alkaloids was found in 10 of the 14 contaminated samples. Only in sample 14, which contained 100% fennel, no contamination was observed. The TOF method was mainly applied for sample screening, rather than to quantify the PA levels. However, highly contaminated samples could be distinguished by the signal intensity. The highest levels of contamination were found in samples (1, 2, 4 and 6, respectively rooibos, mint, chamomile and a combination of mint and fennel). Mass spectra of the 15 analysed samples, are displayed below (***Figure 4.3***).

Table 4.2

Detected alkaloids in each of the 15 analysed tea samples.

Sample	Contaminating alkaloids
1	echinatine, echinatine N-oxide, lasiocarpine
2	integerrimine, seneciphylline N-oxide, integerrimine N-oxide
3	echinatine, heliotrine, integerrimine N-oxide, echimidine N-oxide
4	echinatine, heliotrine, integerrimine N-oxide, echimidine N-oxide
5	echinatine, heliotrine
6	lasiocarpine, lasiocarpine N-oxide
7	heliotrine, integerrimine N-oxide, echimidine N-oxide
8	echinatine
9	europine
10	echinatine, heliotrine, echimidine N-oxide
11	echinatine
12	heliotrine, echimidine N-oxide
13	echinatine, echinatine N-oxide
14	NO CONTAMINATION
15	seneciphylline

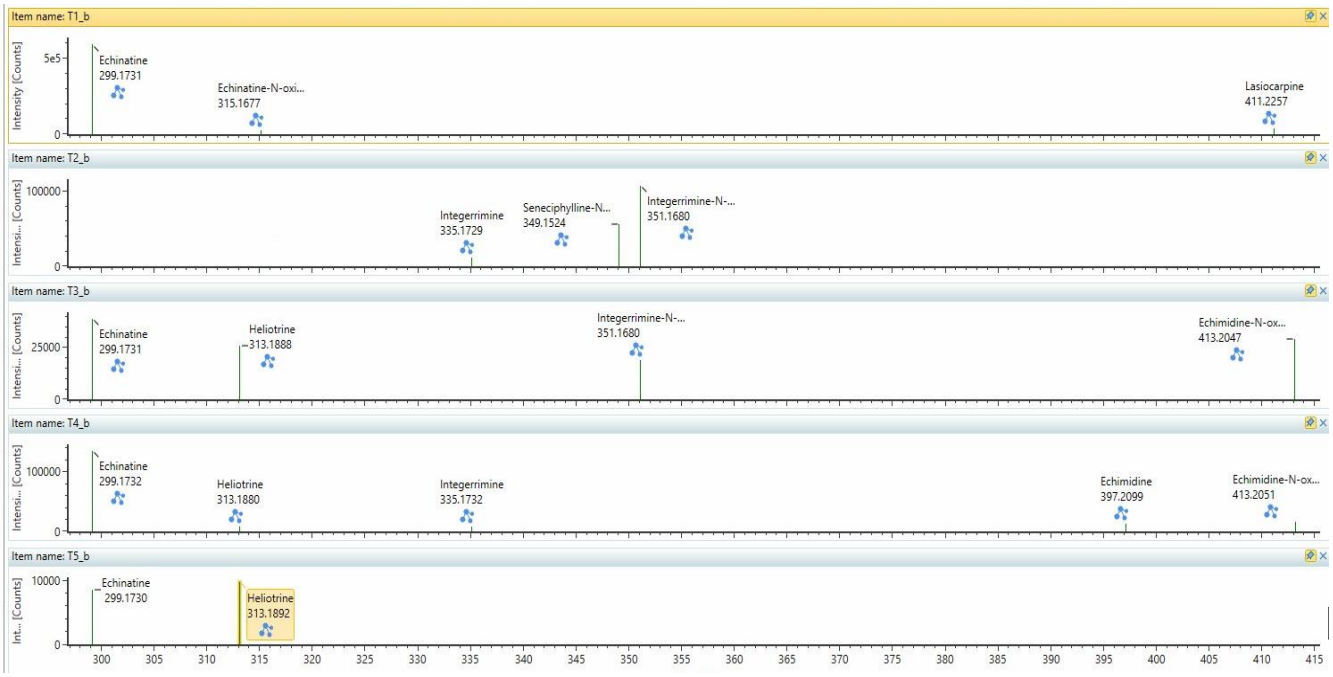

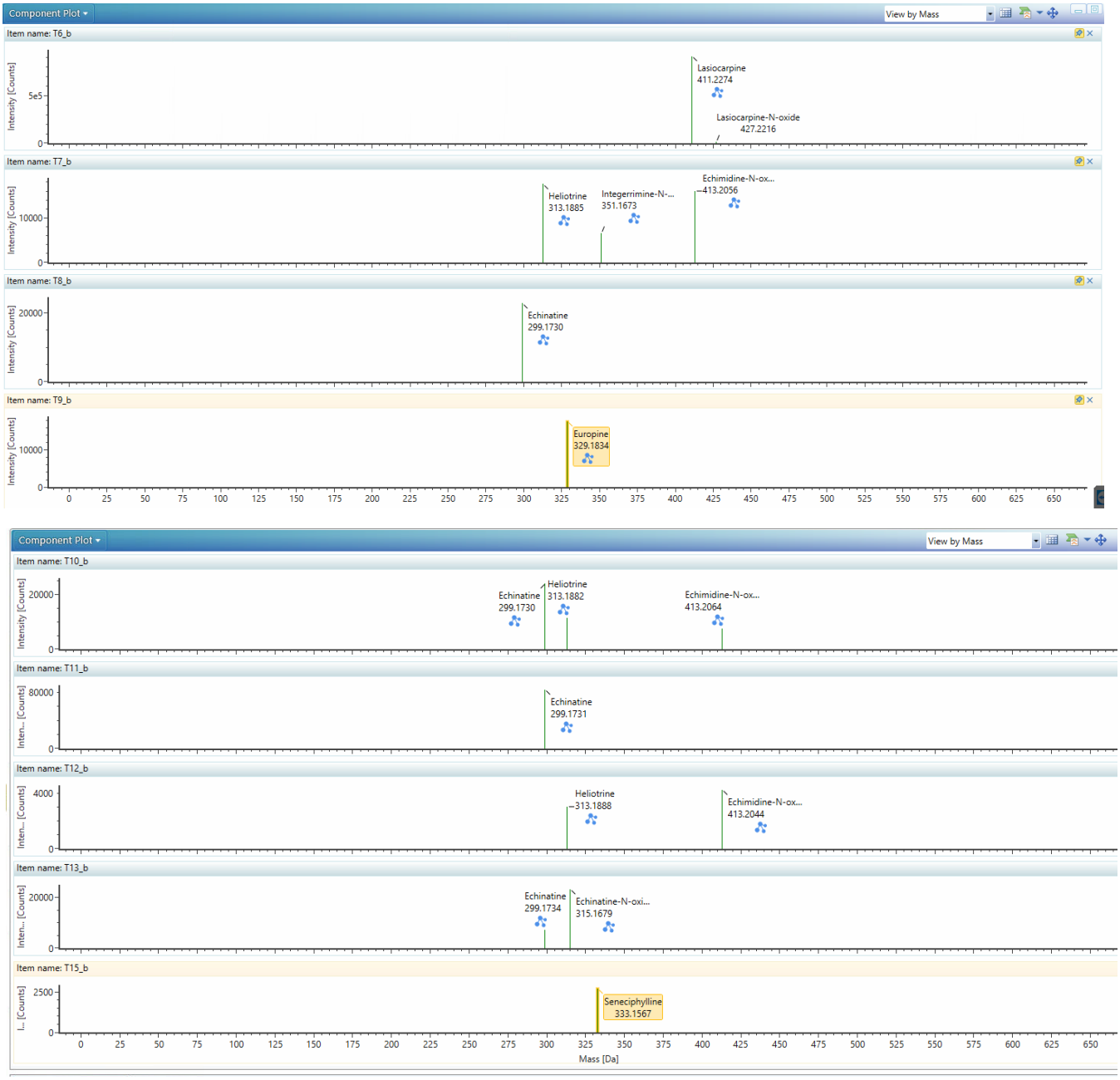

Figure 4.3

Mass spectrometry information of the 15 analysed tea samples, screened with a Vion IMS TOF mass spectrometer. The contaminating alkaloids are identified for each sample.

The first sample containing a mixture of rooibos and mint, is displayed in more detail below (***Figure 4.4***). Product information of all the analysed samples, can be found in (***Table 3.2***) in attachments. A specific identification for each PA present in the sample, was given by the device. The identification was three-dimensional, based on RT (chromatograms), *m/z* values (molecular weights) and drift time. The complete

fragmentation pattern of each molecule, provided an additional identification certainty. Thanks to the combination of this parameters, every contaminant in the samples was identified.

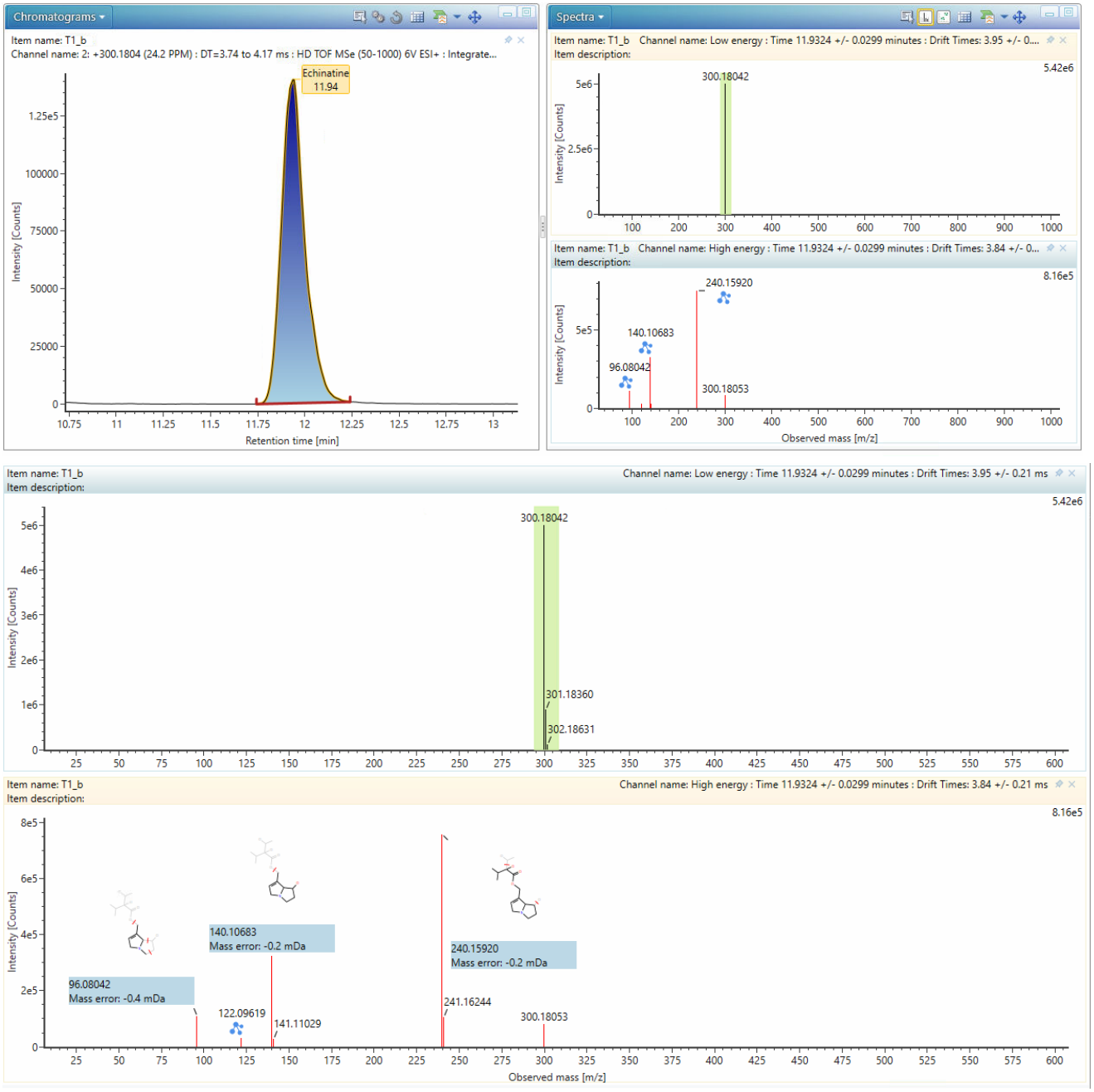

Figure 4.4

Three-dimensional identification of sample 1.

Retention time, drift time and a complete fragmentation pattern is given for echinatine.

4.2. COLLISION CROSS-SECTION DATABASE

Two different platforms, *CCSbase* and *AllCCS*, based on machine learning were applied to predicted CCS values for targeted alkaloids. This work provided the first traveling-wave IMS (TWIMS)-derived CCS library for the 35 EU-regulated PAs. *AllCCS* provided information for $[M+H]^+$, $[M+H-H2O]^+$, $[M+Na]^+$, $[M+NH4]^+$, $[M-H]^-$, $[M+Na-2H]^-$, $[M+HCOO]^-$. *CCSbase* did not reported the $[M+H-H2O]^+$, $[M+HCOO]^-$ ions. The experimentally observed CCS values were obtained by injecting two different concentrations of each PA standard into the device. The CCS values hardly differed between the two concentrations. The robustness of CCS was proven, by the consistent results across different concentration levels. This makes CCS a good additional molecular identifier. (***Table 4.5***) in attachments, displays specific information as neutral mass, observed neutral mass, *m/z* ratio and mass error for each of the analyzed alkaloids.

Experimentally observed CCS values, were obtained for the most abundant ion $[M+H]^+$ of each PA. The mean CCS across the different concentrations, was used to compare experimental and theoretical results. A prediction error was calculated separately for each of the 35 PAs, obtained with both algorithms. The mean prediction error of the database created by *AllCCS* was 1.12 %. A mean prediction error of 2.20% was reported for the *CCSbase* predictions. The prediction error of a reliable database should not be higher than 2% (60). Therefore it can be concluded, that the predictions based on *AllCCS,* were accurate, and met the imposed limits. The prediction error of 2.20% for the library based on CCSbase, was slightly outside the 2% criteria. (***Table 4.6***) in attachments gives a complete overview of the created CCS library, as well as experimentally obtained values. Specific prediction errors for both algorithms are displayed.

4.3. TRANSFERING THE TOF METHOD TO A QUANTIFYNG QqQ METHOD

The available screening method, using a time of flight (TOF) analyser was transferred to a less expensive and user-friendly triple quadrupole (QqQ). This new method, will be used for routine quantification of PAs in tea samples. The available TOF method was used as a starting point, for development of a new UPLC-MS/MS protocol. A standard mixture of 21 PAs was used to select the most optimal conditions. 8 different runs were needed before finding the ideal gradient, mobile phases, flow rate, injection volume and collision energy. Especially the gradient caused the most difficulties, and needed several corrections. In this section, the methods which led to important new insights will be discussed in more detail. The attached chromatograms (***Figure 4.7*** in attachments), substantiated the improving quality of the peaks in the different methods, when changing the UPLC/MS-MS conditions.

4.3.1. Method 1

The method of *Dreolin* (66), found in literature was tested. Mobile phase A was composed of: 5 mM ammonium formate in water + 0.1% formic acid (v/v%). Phase B contained: acetonitrile + 0.1% formic acid (v/v%). The injection volume was 5 µL and a flow rate of 0.3 ml/min was applied. The applied gradient of method 1 is displayed in (***Table 4.8***) below. Three different flow rates were compared (0.2, 0.25 and 0.3 mL/min). The influence of the changing pressure on the system was observed. Applying the lower flow rates (0.2 and 0.25 mL/min) a trend of band-broadening appeared. This problem was partially solved by the use of a higher pressure. Therefore, a flow rate of 0.3 mL/min was selected.

Table 4.8

Applied gradient Method 1.

Time (min)	% A (Aqueous)	% B (Organic)
0	95	5
1.0	95	5
12.0	85	15
20.0	65	35
20.5	5	95
22.0	5	95
22.1	95	5
30.0	95	5

Problems/ limitations of the method:

Some isomers were not separatable (intermidine - lycopsamine + their N-oxide forms and senecivernine – senecionine). The alkaloids co-eluted because of their similar chemical structures, which ensured similar retention times. Identification of these compounds was not possible because they had a similar fragmentation pattern. Band-broadening and peak-fronting resulted in a non-ideal peak shape. The first eluting compounds were more subjected to band-broadening compared to those which had a higher retention time. This problem is described in literature, when the concentration of organic solvent is too high at the start of the run. Therefore, the gradient was adjusted in Method 2.

4.3.2. Method 2

Mobile phase A was composed of: 2 mM ammonium formate in water + 0.2% formic acid (v/v%). Phase B contained: methanol 2 mM ammonium formate + 0.2% formic acid (v/v%). The applied gradient of Method 2, is displayed in (***Table 4.9***) below. Given the proven benefit, a flow rate of 0.3 mL/min was chosen. The method was initially performed with an injection volume of 5 µL. Seen the remaining fronting in the majority of the peaks, the injection volume was changed to 3 µL. The peak fronting

was reduced, adjusting this condition. Moreover, because the organic mobile phase was changed to methanol, a better peak shape could be observed, compared to the use of acetonitrile.

Table 4.9

Applied gradient Method 2.

Time (min)	% A (Aqueous)	% B (Organic)
0.0	90	10
8.0	70	30
16.0	40	60
17.0	0	100
19.0	0	100
20.0	90	10
25.0	90	10

Problems/ limitations of the method:

The initial peaks still showed band-broadening, and the same compounds as mentioned in Method 1 co-eluted. In the following methods, different gradients were tested in order to fix this problem. The composition of the mobile phases, the flow rate and injection volume, were kept the same as in Method 2.

4.3.3. Method 3 and 4

In Method 3, the % organic phase B in the first minutes was reduced. The influence of a quicker increase of mobile phase B in the beginning, was checked in Method 4. The exact gradients of all the tested methods, can be found in (***Table 3.7***) in attachments. It was observed that reducing the % of mobile Phase B at the beginning (Method 3), decreased the band-broadening of the initial peaks. So, the following methods were realized, using the same principal as Method 3. Method 4 delivered low quality peak shapes and even increased the band-broadening and tailing. Therefore, this method was not continued.

4.3.4. Method 5

This method started with 100% aqueous mobile phase A. The increase of phase B at the beginning of the run was much faster compared to the previous methods. The results obtained with this method showed improvement in peak-shape and separation. The next three methods (Methods 6, 7 and 8) were proposed to optimize the gradient at the first minutes of the run. The following methods used the same principals as used in Method 5. The exact gradients can be found in (***Table 3.7***) in attachments.

4.3.5. Method 8

This method is the chosen method, that contained the most optimal conditions to separate the different pyrrolizidine alkaloids in the mixture. (***Table 4.10***) below displays the chosen gradient. In the previous methods, a mean collision energy of 30 eV was applied. Once the most optimal method was found, the specific collision energies for each compound could be applied. An overview of the specific collision energies can be found in (***Table 3.8***) in attachments. The specific collision energies made it possible to identify the compounds with more certainty. Because of the fragment ions, compounds with similar retention times can be distinguished from each other. When the pure standards of the 21Pas will be available in the lab, collision energies will be even more specialized for each fragment.

Table 4.10

Applied gradient method 8 (most optimal method).

Time (min)	% A (Aqueous)	% B (Organic)
0.0	100	0
1.0	90	10
2.0	90	10
6.0	80	20
7.0	60	40
13.0	50	50

15.0	40	60
16.0	0	100
18.0	0	100
19.0	100	0
25.0	100	0

Using this method, 18 of the 21 alkaloids were efficiently baseline separated within 25 min. Method 8 was able to separate multiple isomers, of which the co-elution was unavoidable in previous methods. The earlier problematic compounds (senecionine, senecivernine and intermidine), obtained qualitative peak shapes, when applying this method. However, co-elution could not be avoided for the following isomers; Lycopsamine, intermedine N-oxide and senesivernine N-oxide. Therefore, this method needs further optimalisation in the future.

(**Table 4.11**) in attachments, gives an overview of mass spectrometry and liquid chromatography information of PAs, collected from different sources. Retention times, precursor and fragment ions are displayed in the table. Thanks to the extra information pooled from literature, the peaks from the mixture could be identified with more certainty.

5. DISCUSSION

5.1. SAMPLE SCREENING USING IMS TOF MASS SPECTROMETRY

5.1.1. Extraction methods

An ion mobility spectrometry (IMS) protocol, using a time of flight (TOF) analyser was already disposable in the laboratory. The available extraction, was based on a chemically complex solid-liquid extraction (SLE) protocol. Plant based samples such as herbs and spices, mostly contain high concentrations of unwanted materials. Therefore, SLE is often applied to eliminate a portion of the matrix co-extractives and reduce the contamination of the system. However, literature indicated that remaining matrix would not be a problem for the TOF analyser (8,67). Therefore, a new liquid-liquid extraction (LLE) method was searched, to simplify the screening protocol.

Acetic acid and formic acid are commonly used to perform LLE (8,66,68). Both of them, are weak acids and were supposed to give similar results. Therefore, only formic acid extraction was tested. Good results and clear extracts, were obtained using the simple formic acid extraction. These results gave a first indication, that a more advanced extraction method is not necessary, seeing the high resolution and selectivity of the IMS TOF analyser.

5.1.2. Sample screening

The analytical TOF strategy was applied to screen 15 commercially available tea samples, bought in Conad, a local Italian marked. The samples were screened for the 35-Eu regulated pyrrolizidine alkaloids (PAs). Of course, there were too few samples to draw a statistical conclusion for the whole market. These test were mainly performed to get a first idea about the contamination problem, and to get the opportunity to work with a TOF analyser.

The TOF method was applied to screen, rather than quantifying the tea matrices. Although, the highly contaminated samples were distinguished by the signal intensity. Multiple PAs and their corresponding PANOs were detected in 14 of the 15 analysed samples. Articles (67,69,70) also reported alkaloids in the majority of the

analysed matrices, which clarified the high number of contaminated samples in this work. The highest contamination was found in rooibos, melissa, chamomile and mint.

Article (68), screened 50 different tea samples, PA contamination was only reported for chamomile and mint. The chamomile samples were mainly contaminated with echimidine N-oxide and retrorsine. The analysed chamomile samples in this work, were in line with article (68), since echimidine N-oxide was the most reported alkaloid. The mint samples in this work, were predominantly contaminated with seneciphylline (N-oxide) and heliotrine, which was confirmed by (68) article as well. The high signal intensity of the rooibos and melissa, was also reported in literature. Article (71), noted PAs in 100% of the analysed rooibos and melissa samples, containing the highest of all concentrations.

Fennel tea was the only blank sample in this study. Fennel for infusion, are the dried seeds from the fennel herb. The seeds remain in the soil until harvesting, therefore the contact with other plants is minimal. As explained before, PAs are mainly present in the prominent tissues of the plant, such as leaves or flowers. For this reason, fennel cross-contamination is rare. Fennel contamination occurs mostly after harvesting during the manufacturing process. The obtained fennel results were completely in line with other articles (68,71), in which the reported PAs were under the LOD for the majority of the fennel samples.

In green tea, a very low signal intensity was obtained for seneciphylline. This sample contained the lowest of all PA concentrations. Green tea grows in a separate bush, therefore cross-contamination is less prevalent. The low contamination rate of green tea is a constant within literature. All the analysed green tea samples in article (67), were below the recommended daily intake for a 60 kg person (210 µg/kg).

No statistical conclusion can be drawn from these results, seen the low number of analysed samples was not representative for the whole marked. Nevertheless, the number of contaminated samples was remarkably high. 14 Of the 15 analysed samples contained a combination of PAs, which were in line with literature findings. Therefore, the results gave a first indication that the worldwide concern around this topic is justified. The significant outcome proved the need for more efficient and

specific identification methods within the food safety field, to which this master scription contributed.

5.2. ION MOBILITY-DERIVED COLLISION CROSS-SECTION DATABASE

Ion mobility could improve the analytical performance of current LC-MS workflows. It is a powerful technique, which improves peak resolution of isomeric and isobaric compounds. Seen the related chemical structures of PAs and the multiple isomers, this approach could offer an additional separation dimension. The application of IMS in the food analytical field has increased considerably over the last years. Nevertheless, the lack of CCS databases for food contaminants still slows down the implementation of this parameter in food safety. This scription provided the first IMS-derived CCS database for the 35 Eu-regulated PAs. This created library, could help to analyse and identify the alkaloids with more certainty. Since theoretical predictions for PAs have never been reported before, no literature was available to compare the results with.

5.2.1. Collision cross-section database

Collision cross-section (CCS) is an additional molecular identifier, based on the chemical structure and three-dimensional conformation of the ion (62). CCS offers additional resolution, next to retention times and *m/z* values. To produces CCS values on a large scale, machine-learning approaches have recently been emerged as a predictive tool. These algorithms learned the relationship between experimental CCS values and molecular descriptors, through a training dataset (72).

CCSbase and *AllCCS* were the two machine-learning models, used to complement the experimental CCS data. The platforms applied the molecular descriptor Simplified molecular-input line-entry (SMILE) to provide a prediction of CCS values. While *AllCCS* provided information for $[M+H]^+$, $[M+H-H2O]^+$, $[M+Na]^+$, $[M+NH4]^+$, $[M-H]^-$, $[M+Na-2H]^-$, $[M+HCOO]^-$. *CCSbase* did not reported the $[M+H-H2O]^+$, $[M+HCOO]^-$ ions.

5.2.2. Prediction error

Theoretical CCS predictions, obtained by the two algorithms (*AllCCS and CCSbase*), were correlated with experiment values. The observed values, were captured by injecting a standard of every alkaloid into the IMS TOF analyser. The standards were injected in two different concentrations, whereafter the mean observed CCS was calculated for each PA. This value, was only displayed for the most abundant ion $[M+H]^+$. In order to assess the accuracy of the theoretical predictions, they were compared with observed CCS values.

Literature indicated that, an overall prediction error of 2%, can be considered as a good-fit criteria (60). The mean prediction error for the created *AllCCS* database was 1.12%. Predictions made by *CCSbase*, had a mean prediction error of 2.20%. It can be conclude that *AllCCS*, provided an accurate prediction of the CCS values and was in compliance with the predetermined limits. *CCSbase* does not completely satisfy the criteria. This bias, could be reduced by feeding the model with more experimental data in the near future (73). As mentioned before, IMS is not yet fully exploited within the food analytical field. A PA database has never been reported before. Therefore, the obtained results could not yet be supported by literature.

5.2.3. Consistency between concentrations

Two different concentrations of each PA standard, were injected into the Vion IMS QTOF analyser. No significant difference was found across the injected concentrations. These results indicated, that CCS values were conserved between different dilutions. The outcome confirmed the benefit of CCS alongside the traditional molecular identifiers of retention time, accurate mass, isotopic pattern, precursor ion and fragment ions (72). Different literature sources reported the same conclusions. Multiple articles conformed consistent CCS measurements between instruments, matrices, laboratories and experimental conditions (59,60,62). These findings substantiated the additional identification benefit of a CCS database.

5.2.4. Limitations

Current liquid chromatography-mass spectrometry workflows, could potentially being improved by IMS. However, article (73) could not report a potential benefit of CCS information for the determination of ergot alkaloids (EAs). Similar to PAs, EAs have related chemical structures, which show analogous fragmentation patterns. Regardless the molecular ion from which they were originated, similar CCS values were obtained for fragment ions with the same *m/z*. The article explained this due to the fact that after fragmentation, isomeric properties are not conserved for EAs. Despite the CCS values could not offer an additional value for EA determination, a CCS database could help identification and recognition of non-targeted compounds. On the other hand, articles (60,72) reported the successful application of CCS values for the determination of targeted pesticides and mycotoxins in food samples.

5.3. DEVELOPMENT OF A NEW QUADRUPOLE UPLC-MS/MS METHOD

A TOF method was already operatable in the laboratory, to screen PAs in tea samples. There was a need to transfer this method to a user-friendly triple quadrupole (QqQ) analyser, to perform routine quantification. The available TOF protocol, was used as a starting point, to develop the new method. The aim was to be able to quantify and identify 21 alkaloids in a standard mixture. The method will be expanded to a larger range of PA in the future, when the analytical standards will be available in the laboratory. In the first stages of development, detection parameters were selected and optimised. Especially the mobile phases, injection volume, flow rate, gradient programme and collision energies were optimised during different runs.

The LC-MS/MS device was used by multiple research groups within the university. Additionally, the QqQ analyser was inoperative for 4 weeks. For this reason, the time to perform analysis was limited. Only an initial exploration could be performed, the method will be further optimised and validated in the near future.

5.3.1. Liquid-chromatography conditions

Separation was achieved using a ACQUITY UPLC BEH™ C8 (2.1 mm × 100 mm, 1.7 µm). A review of literature yielded that a shorter column for example (2.1 mm x 50 mm, 2.5 µm), was able to deliver satisfactory results for a low number of PAs. When the scope of the research was expanded to the associated PANOs, band broadening and asymmetrical peaks were observed (68). The aim of this research was, to be able to detected both PAs and PANOs, therefore a longer column was preferred. Reversed phase liquid chromatography was selected as the best technique to analyses PAs and PANOs. This approach was consistent with previous articles (66,74).

The influence of mobile phase ingredients on chromatographic parameters, was also investigated during research. The main ingredient of the mobile phase was water, both acetonitrile and methanol were tested as organic modifiers. When using acetonitrile, like suggested in (27,66), the peak quality and separation was not as beautiful as described in the article. The use of acetonitrile as organic phase, resulted in a co-elution of Intermedine – lycopsamine + their N-oxides, senecivernine and senecionine had similar RT as well.

In article (75) no satisfactory chromatographic resolution could be achieved when using acetonitrile. The article reported exactly the same problematic co-eluting compounds as observed in this study. To optimize separation, this source changed the organic phase to methanol and obtained an improved baseline separation for four of the co-eluting compounds. Based on this article (75), the organic phase was changed from acetonitrile to methanol. The use of methanol increased the peak symmetry and separation. With a view to developing a routine technique, methanol had the advantage of being a less costly solvent.

Literature indicated that a significant factor contributing to the effectiveness of ionization, was the addition of an acidic modifier to the mobile phase (66,74–76). A suitable mobile phase additive can modify the chromatographic separation and even improve the analytes detectability. The signal intensity of the majority of the peaks was improved when 2 mM ammonium formate and 0.2% formic acid was applied. The addition of an acidic modifier resulted in significant growth of the detector's signal.

Obtained results justify the selection of acidic additional ingredient to the mobile phases.

In multiple articles, a rather high injection volume is used, varying between 5-10 µL (66–68). When applying injection volumes of 5 µL, fronting was a remaining problem. A possible explanation could be the wear and frequent use of the UPLC-MS/MS device. The optimal injection volume could also be influenced by a combination of other applied parameters. Better peak shapes were obtained when using an injection volume of 3 µL. Thereafter, three different flow rates were investigated (0.2, 0.25 and 0.3 mL/min). In literature (27,67,69), the highest flow rates were the most successful. Different runs provided consistent results as previous publications. Applying a higher pressure, the compounds were eluting faster from the column. This way, less tailing and suboptimal peak shapes were observed.

Gradient elution was necessary to achieve proper separation of the mixture of PAs and PANOs. Several modifications of the gradient program, involving reducing or increasing the initial concentration of the organic modifier, were tested. When applying a gradient based on the principles of the initial reference method (66), no similar peak shapes and separation, as described in the article could be obtained. The recurring problem was the band-broadening of the first eluting compounds, compared to those with a higher retention time.

This problem was described in literature when the concentration of organic solvent used in the beginning is too high. It was observed that reducing the % of the organic modifier at the beginning, decreased the band-broadening of the initial peaks. Optimalisation especially at the first minutes of the run, eventually resulted in a segmented gradient with flattened slopes. This gradient achieved the best possible separation of the target compounds. A similar segmented gradient approach delivered good separation results in previous publications (75).

5.3.2. Mass spectrometry conditions

The first aspect considered, was the most appropriate method of ionisation. Literature review indicated, that electron spray ionisation (ESI) delivered significantly higher intensity in comparison to atmospheric pressure ionisation (API). Since ESI

yielded the greatest intensity of signals (both peak hight and surface area), it was chosen. The same favourable results as in similar studies were obtained, using this method of ionisation (66–68,74). Selection of the best ion creation mode, was also not without importance. Positive ion registration mode was applied, seen the much better results obtained in literature. The influence of a negative ionisation mode was not investigated during this research. Working in full scanning mode, parent ion and fragmentation ion transitions were proposed for every compound. This approach significantly improved the credibility and unambiguous identification of the analytes.

The collision energies (CE) were optimised to get an improved ion intensity. The available standard mixture contained a small amount of matrix, which disrupted the automatic function of the device. Therefore, the collision energies were chosen manually based on information found in literature. To select the collision energies, the principals explained in article (68) were followed. Setting a low collision energy value, leads to the creation of fragment ions of greater molecular weights. On the other hand, increasing CE resulted in increased signal intensity of fragment ions of lower molecular weights.

5.3.3. Isomeric alkaloid separation

The biggest challenge encountered in this study, was undoubtedly the chromatographic baseline separation of the isomers. The chemical structures of PAs are closely related, therefor they have the similar precursor and product ions. Especially isomers with one or more identical mass transition are hard to resolve under RPLC conditions. Using the optimised separation described above, baseline separation was achieved for 18 of the 21 alkaloids, based on mass fragmentation differences and RT. 3 coeluting isomers could not be separated, and should be quantified as sum. Although a slow RPLC gradient and U-HPLC column were employed, a full spectral resolution of some isomers could not be achieved under any conditions.

Several other studies reported difficulties to distinguish the co-eluting isomers using a quadrupole UPLC-MS/MS method (11,66,74,75,77). In article (66), similar UPLC-MS/MS conditions (column, gradient, mobile phases) were used. Baseline

separation could not be obtained for the following isomers; Lycopsamine, intermedine and senesivernine N-oxide. The same problematic isomers were seen in this current study. Optimised UPLC-MS/MS conditions could not improve co-elution.

Article (75), encountered similar co-elution problems of multiple groups of isomeric alkaloids (intermedine, lycopsamine and their corresponding PANOs). These analytes could not be resolved chromatographically nor spectrometrically under any of the tested conditions. In this article, an alternative separation represented by hydrophilic interaction liquid chromatography (HILIC) was proposed as solution. The sample separation in a second chromatographic system, provided an optimised separation selectivity. All the problematic co-eluting isomers could be fully separated using the HILIC system. Given the favorable results obtained in this article, the HILIC approach could be a possible solution to separate the co-eluting isomers.

Because of the remaining co-eluting problem, the EU regulation has set maximum limits for the sum of PAs, rather than limits for individual compounds. Quantification was considered as the sum of both analytes, for co-eluting isomers. The well-known problem of the inappropriate resolving of isomers, possibly results in analyte overestimation. The phenomenon of overestimation is often neglected in literature. Therefore, the new EU legislation for the sum of PAs and PANOs was re-evaluated at European level (78).

5.4. VALIDATION PROCEDURE

When the developed triple quadrupole method is fully optimised and ready to use, a scientific validation will be performed. Validation is a necessary process, which establish scientific evidence that the developed method is capable to deliver qualitative results in a consistent way. Method validation is usually performed, using artificially contaminated blanks. Literature suggests to obtain a pure blank for different types of tea (66). Differences in the amount of matrix effects can be expected between commodities, as well as in individual samples of the same type. In the further development of this project, a database of blanks will be established for a large collection of regulated tea matrices. Method trueness, limit of quantification (LOQ),

Limit of detection (LOD), recoveries and repeatability are commonly reported validation parameters. Thereafter, the validation parameters will have to comply with the required ranges for qualitative methods of analysis, set out by the European Commission Decision 2002/657/EC.

5.5. FUTURE RESEARCH

Pyrrolizidine alkaloids rise more and more attention in the food analytical field. Seen their carcinogenic and genotoxic properties, there is a need to continue extensive research. The following section describes some potential additional investigations, which are related to this master scription.

5.5.1. Enlarge the IMS-derived CCS database

The implementation of IMS within the food safety field is quite new. To speed up the IMS applicability within the food analysis, there is a need of more CCS databases. Up to now, very few contaminant databases have been proposed. The available libraries are far from covering the broaden range of contaminants in the food chain. In the future, the created CCS database could be expanded for a larger range of PAs. By comparing experimentally obtained and theoretical CCS values, a higher degree of confidence in the identification of both new and targeted PAs could be provided.

5.5.2. Simultaneous analysis of tropane alkaloids

Literature indicates that similar extraction methods and UPLC-MS/MS conditions could be used to analyze tropane alkaloids (TAs) (3,8,13). These plant toxins are another class of frequently reported substances in herbal tea. TAs are extremely toxic, therefore EFSA has set maximum limits for atropine and scopolamine. Other studies have already succeed developing a method for simultaneous determination of both PAs and TAs (74,76). Similar analyzing techniques, using a weak acid for simple liquid-liquid extraction and methanol as organic modifier, are suggested in literature. Thanks to some small adaptations to the collision energies and

gradient, the method could be used to additionally analyze TAs. The possibility to analyze both PAs and TAs with the same method, would be a great added value to the developed method.

5.5.3. Influence of tea infusion on the PA levels

Research into the difference in PA levels between tea infusion and solid tea leaves, could be another addition to this research. In this current master scription, only solid tea leaves were extracted to perform analysis. It could be interesting to compare the PA levels with the levels found in tea infusions, since tea is never consumed in its solid form. PAs are a relatively heat-stable type of toxin, it might be a good addition to investigate the influence of boiling water.

6. CONCLUSION

The first goal of this work was to get an idea about the PA contamination in different tea matrices. Therefore, 15 tea samples were screened in duplicate. An IMS QTOF mass spectrometry protocol, was already operatable in the laboratory. However, a novel extraction method was searched in literature, to simplify the process. A simple formic acid liquid-liquid extraction method, effectively isolated PAs from dried herbs. Of course, the low number of analyzed samples was not representative for the whole marked. Nevertheless, the number of contaminated samples was remarkably high. In 14 of the 15 analysed samples, PA contamination was detected. The detected PAs in the different tea matrices, matched literature findings. Therefore, the results gave a first indication that the worldwide concern around this topic is justified. The significant outcome proved the need for more efficient identification methods within the food safety field.

Ion mobility spectrometry (IMS) with high resolution mass spectrometry (HRMS) has become an important tool, to screen both targeted and non-targeted compounds. Nevertheless, this approach still remains quite unexplored in food safety. The lack of CCS databases for contaminants, is the main problem of the slow IMS implementation. This scription provided the first Traveling-wave IMS (TWIMS)-derived CCS database for the 35 Eu-regulated PAs. Theoretical CCS data were obtained by two analytical algorithms, trained with machine learning. As a proof of concept, experimentally-derived and theoretical values, were compared by calculating a prediction error. A mean prediction error of 1.12% was obtained for *AllCCS* results, which was in compliance with the imposed limit of 2%. The mean prediction error obtained by *CCSbase* was 2.20%, this value felt slightly outside the criteria. It can be concluded that both databases are reliable and can be used as an additional tool for compound identification.

Seen the limited availability, high complexity and cost, there was a need to transfer the screening TOF method to a more assessable and user-friendly triple quadrupole (QqQ) method. In present study, the first exploration of a novel and fast protocol was described for the determination of 21 pyrrolizidine alkaloids. Different device parameters were tested in order to select the most optimal conditions.

Both acetonitrile and methanol were tested as organic modifiers. When using acetonitrile, the separation was not optimal and multiple components were problematic. Methanol was preferred, because it increased the peak symmetry and separation of the compounds. The signal intensity of the majority of the peaks was improved when 2 mM ammonium formate and 0.2% formic acid were applied as acidic modifiers. When the injection volume was reduced form 5 µL to 3 µL, the band-broadening decreased and the peak quality improved. Additionally, different flow rates were investigated (0.2, 0.25 and 0.3 mL/min). The highest pressure, resulted in less tailing and better peak shapes. Several modifications of the gradient, were tested. The recurring problem was the band-broadening of the first eluting compounds. Optimalisation especially at the first minutes of the run, eventually resulted in a segmented gradient with flattened slopes. The available standard mixture contained a small amount of matrix, which disrupted the automatic collision function of the device. Therefore, the collision energies were chosen manually, based on literature.

18 of the 21 PAs in the standard mixture were baseline separated efficiently within 25 min. During the optimalisation of the UPLC-MS/MS conditions, the separation, peak shapes and intensity of the compounds improved. Co-elution could not be avoided for the following isomers; Lycopsamine, intermedine N-oxide and senesivernine N-oxide. Other articles reported the same problematic co-eluting compounds, without a proper solution to this problem. In further stadia of this research, the method will be further optimised to separate the co-eluting isomers.

The initial objectives of this master scription have been achieved. 15 Samples were successfully screened for PAs using a TOF method. This scription provided the first IMS-derived CCS database for PAs, of which the additional value was confirmed by the low prediction errors. Additionally, the available TOF method was transferred to a more simple QqQ protocol, to perform quantification. This work contributed, to the first stages of developing an UPLC-MS/MS method, using a QqQ analyzer. The co-elution of the following isomers; Lycopsamine, intermedine and senesivernine N-oxide, was unavoidable. Therefore, this method needs further optimalisation in the future.

The worldwide concern and interest around this topic is justified by the increasing reports of PA contamination. In terms of global trade and food safety, both accessible routine quantification as well as more advanced screening techniques using CCS databases, should get more attention. This way it could prevent contaminated tea to enter the market and cause a serious risk to human health.

7. REFERENCES

1. Bhambhani S, Kondhare KR, Giri AP. Diversity in Chemical Structures and Biological Properties of Plant Alkaloids. Molecules [Internet]. 2021 Jun 3 [cited 2023 Feb 17];26(11):3374. Available from: https://www.mdpi.com/1420-3049/26/11/3374
2. Shitan N, Kato K, Shoji T. Alkaloid transporters in plants. Plant Biotechnology [Internet]. 2014;31(5):453–63. Available from: https://www.jstage.jst.go.jp/article/plantbiotechnology/31/5/31_14.1002a/_article
3. Dzuman Z, Jonatova P, Stranska-Zachariasova M, Prusova N, Brabenec O, Novakova A, et al. Development of a new LC-MS method for accurate and sensitive determination of 33 pyrrolizidine and 21 tropane alkaloids in plant-based food matrices. Anal Bioanal Chem. 2020 Oct 1;412(26):7155–67.
4. Matsuura HN, Fett-Neto AG. Plant Alkaloids: Main Features, Toxicity, and Mechanisms of Action. Plant Toxins [Internet]. 2015 [cited 2023 Feb 27];1–15. Available from: https://link.springer.com/referenceworkentry/10.1007/978-94-007-6728-7_2-1
5. War AR, Paulraj MG, Ahmad T, Buhroo AA, Hussain B, Ignacimuthu S, et al. Mechanisms of plant defense against insect herbivores. https://doi.org/104161/psb21663 [Internet]. 2012 [cited 2023 Feb 27];7(10):1306–20. Available from: https://www.tandfonline.com/doi/abs/10.4161/psb.21663
6. Christiansen JL, Joørnsgård B, Buskov S, Olsen CE. Effect of drought stress on content and composition of seed alkaloids in narrow-leafed lupin, Lupinus angustifolius L. European Journal of Agronomy. 1997 Dec 1;7(4):307–14.
7. Wojtyczka RD, Dziedzic A, Kępa M, Kubina R, Kabała-Dzik A, Mularz T, et al. Berberine Enhances the Antibacterial Activity of Selected Antibiotics against Coagulase-Negative Staphylococcus Strains in Vitro. Molecules 2014, Vol 19, Pages 6583-6596 [Internet]. 2014 May 22 [cited 2023 Feb 27];19(5):6583–96. Available from: https://www.mdpi.com/1420-3049/19/5/6583/htm
8. González-Gómez L, Morante-Zarcero S, Pérez-Quintanilla D, Sierra I. Occurrence and Chemistry of Tropane Alkaloids in Foods, with a Focus on Sample Analysis Methods: A Review on Recent Trends and Technological Advances. Foods [Internet]. 2022 Jan 30 [cited 2023 Feb 22];11(3):407. Available from: https://www.mdpi.com/2304-8158/11/3/407
9. Wink M. Alkaloids: Toxicology and Health Effects. Encyclopedia of Food and Health [Internet]. 2016 Jan 1 [cited 2023 Feb 27];106–14. Available from: https://linkinghub.elsevier.com/retrieve/pii/B9780123849472000209
10. Cirlini M, Cappucci V, Galaverna G, Dall'Asta C, Bruni R. A sensitive UHPLC-ESI-MS/MS method for the determination of tropane alkaloids in herbal teas and extracts. Food Control. 2019 Nov 1;105:285–91.
11. Mulder PPJ, Sánchez PL, These A, Preiss-Weigert A, Castellari M. Occurrence of Pyrrolizidine Alkaloids in food. EFSA Supporting Publications. 2017 Mar 7;12(8).
12. Adamse P, van Egmond HP, Noordam MY, Mulder PPJ, de Nijs M. Tropane alkaloids in food: poisoning incidents. https://doi.org/103920/QAS20130314

[Internet]. 2014 Jan 28 [cited 2023 Feb 27];6(1):15–24. Available from: https://www.wageningenacademic.com/doi/10.3920/QAS2013.0314
13. Kohnen-Johannsen KL, Kayser O. Tropane Alkaloids: Chemistry, Pharmacology, Biosynthesis and Production. Molecules 2019, Vol 24, Page 796 [Internet]. 2019 Feb 22 [cited 2023 Feb 27];24(4):796. Available from: https://www.mdpi.com/1420-3049/24/4/796/htm
14. Dusemund B, Rietjens IMCM, Cartus A, Schaefer B, Lampen A. Pflanzliche Kontaminanten in Lebensmitteln: Vorkommen, Wirkung und Risikobewertung. Bundesgesundheitsblatt Gesundheitsforschung Gesundheitsschutz [Internet]. 2017 Jul 1 [cited 2023 Feb 28];60(7):728–36. Available from: https://link.springer.com/article/10.1007/s00103-017-2561-6
15. Moreira R, Pereira DM, Valentão P, Andrade PB. Pyrrolizidine Alkaloids: Chemistry, Pharmacology, Toxicology and Food Safety. International Journal of Molecular Sciences 2018, Vol 19, Page 1668 [Internet]. 2018 Jun 5 [cited 2023 Mar 24];19(6):1668. Available from: https://www.mdpi.com/1422-0067/19/6/1668/htm
16. Casado-Hidalgo G, Morante-Zarcero S, Pérez-Quintanilla D, Sierra I. Opium alkaloids in food products: Current and future perspectives. Trends Food Sci Technol. 2021 Feb 1;108:92–102.
17. Mulac D, Humpf HU. Cytotoxicity and accumulation of ergot alkaloids in human primary cells. Toxicology. 2011 Apr 11;282(3):112–21.
18. Scientific Opinion on Pyrrolizidine alkaloids in food and feed. EFSA Journal [Internet]. 2011 Nov 1 [cited 2023 Mar 8];9(11). Available from: https://www.efsa.europa.eu/en/efsajournal/pub/2406
19. Scientific Opinion on Pyrrolizidine alkaloids in food and feed. EFSA Journal. 2011 Nov 1;9(11).
20. Dietary exposure assessment to pyrrolizidine alkaloids in the European population. EFSA Journal. 2016;14(8).
21. Dietary exposure assessment to pyrrolizidine alkaloids in the European population. EFSA Journal. 2016;14(8).
22. Knutsen HK, Alexander J, Barregård L, Bignami M, Brüschweiler B, Ceccatelli S, et al. Risks for human health related to the presence of pyrrolizidine alkaloids in honey, tea, herbal infusions and food supplements. EFSA Journal. 2017 Jul 1;15(7).
23. NEW MAXIMUM LEVELS OF PYRROLIZIDINE ALKALOIDS | Food Compliance Solutions [Internet]. [cited 2023 Mar 8]. Available from: https://regulatory.mxns.com/en/new-maximum-levels-pyrrolizidine-alkaloids
24. Dey P, Kundu A, Kumar A, Gupta M, Lee BM, Bhakta T, et al. Analysis of alkaloids (indole alkaloids, isoquinoline alkaloids, tropane alkaloids). Recent Advances in Natural Products Analysis. 2020 Jan 1;505–67.
25. Lichman BR. The scaffold-forming steps of plant alkaloid biosynthesis. 2021;
26. Keuth O, Humpf HU, Fürst P. Determination of pyrrolizidine alkaloids in tea and honey with automated SPE clean-up and ultra-performance liquid chromatography/tandem mass spectrometry. Food Addit Contam Part A Chem Anal Control Expo Risk Assess [Internet]. 2022 [cited 2023 Feb 28];39(1):149–57. Available from: https://www.tandfonline.com/action/journalInformation?journalCode=tfac20

27. Chung SWC, Lam CH. Development of an Analytical Method for Analyzing Pyrrolizidine Alkaloids in Different Groups of Food by UPLC-MS/MS. J Agric Food Chem [Internet]. 2018 Mar 21 [cited 2023 Feb 27];66(11):3009–18. Available from: https://pubs.acs.org/doi/abs/10.1021/acs.jafc.7b06118
28. Kwon Y, Koo Y, Jeong Y. Determination of pyrrolizidine alkaloids in teas using liquid chromatography–tandem mass spectrometry combined with rapid-easy extraction. Foods [Internet]. 2021 Oct 1 [cited 2023 Feb 28];10(10):2250. Available from: https://www.mdpi.com/2304-8158/10/10/2250/htm
29. Medicines Agency E. Public statement on the use of herbal medicinal products 1 containing toxic, unsaturated pyrrolizidine alkaloids (PAs) including recommendations regarding contamination of herbal medicinal products with PAs Final Draft discussed by Working Party on Community monographs and. [cited 2023 Feb 27]; Available from: www.ema.europa.eu/contact
30. Chemische structuur van pyrrolizidine-alkaloïden [3, 4] | Wetenschappelijk schema downloaden [Internet]. [cited 2023 Mar 1]. Available from: https://www.researchgate.net/figure/Chemical-structure-of-pyrrolizidine-alkaloids-3-4_fig1_335090707
31. Chan TYK. Worldwide Occurrence and Investigations of Contamination of Herbal Medicines by Tropane Alkaloids. Toxins 2017, Vol 9, Page 284 [Internet]. 2017 Sep 15 [cited 2023 Feb 27];9(9):284. Available from: https://www.mdpi.com/2072-6651/9/9/284/htm
32. Knutsen HK, Alexander J, Barregård L, Bignami M, Brüschweiler B, Ceccatelli S, et al. Risks for human health related to the presence of pyrrolizidine alkaloids in honey, tea, herbal infusions and food supplements. EFSA Journal. 2017 Jul 1;15(7).
33. Coskun O. Separation techniques: Chromatography. North Clin Istanbul [Internet]. 2016 [cited 2023 Mar 2];3(2):156–60. Available from: www.kuzeyklinikleri.com
34. Rusli H, Putri RM, Alni A. Recent Developments of Liquid Chromatography Stationary Phases for Compound Separation: From Proteins to Small Organic Compounds. Molecules 2022, Vol 27, Page 907 [Internet]. 2022 Jan 28 [cited 2023 Mar 2];27(3):907. Available from: https://www.mdpi.com/1420-3049/27/3/907/htm
35. Snyder Kirkland LJ. Introduction to Modern Liquid Chromatography. 1979;
36. Zhao J, Carr PW. An approach to the concept of resolution optimization through changes in the effective chromatographic selectivity. Anal Chem [Internet]. 1999 Jul 15 [cited 2023 Mar 2];71(14):2623–32. Available from: https://pubs.acs.org/doi/full/10.1021/ac981321k
37. Dores-Sousa JL, de Vos J, Eeltink S; Vrije Universiteit Brussel Resolving power in liquid chromatography: A trade-off between efficiency and analysis time. 2019 [cited 2023 Mar 2]; Available from: https://doi.org/10.1002/jssc.201800891
38. Liquid Chromatography - Chemistry LibreTexts [Internet]. [cited 2023 Mar 2]. Available from: https://chem.libretexts.org/Bookshelves/Analytical_Chemistry/Supplemental_Modules_(Analytical_Chemistry)/Instrumentation_and_Analysis/Chromatography/Liquid_Chromatography
39. Afeyan NB, Gordon NF, Mazsaroff I, Varady L, Fulton SP, Yang YB, et al. Flow-through particles for the high-performance liquid chromatographic

separation of biomolecules: perfusion chromatography. J Chromatogr A. 1990 Oct 19;519(1):1–29.
40. Normal and Reversed Phase Chromatography for Reliable Polishing | Biopharmaceutical Manufacturing | Merck [Internet]. [cited 2023 Mar 2]. Available from: https://www.merckmillipore.com/BE/fr/products/biopharmaceutical-manufacturing/downstream-processing/chromatography/reversed-phase-normal-phase-chromatography/WIGb.qB.NyAAAAFAbN5kiQpx,nav?ReferrerURL=https%3A%2F%2Fwww.google.com%2F
41. Weston A, Brown PR. HPLC and CE : principles and practice. 1997;280.
42. Böttcher J, Margraf M, Monks K, Net ; Applications@knauer. HPLC Basics-principles and parameters. [cited 2023 Mar 2]; Available from: www.knauer.net
43. Murayama C, Kimura Y, Setou M. Imaging mass spectrometry: Principle and application. Biophys Rev [Internet]. 2009 Sep 9 [cited 2023 Mar 2];1(3):131–9. Available from: https://link.springer.com/article/10.1007/s12551-009-0015-6
44. Kruve A, Rebane R, Kipper K, Oldekop ML, Evard H, Herodes K, et al. Tutorial review on validation of liquid chromatography-mass spectrometry methods: Part II. Vol. 870, Analytica Chimica Acta. Elsevier; 2015. p. 8–28.
45. Taverniers I, De Loose M, Van Bockstaele E. Trends in quality in the analytical laboratory. II. Analytical method validation and quality assurance. TrAC Trends in Analytical Chemistry. 2004 Sep 1;23(8):535–52.
46. Inleiding tot LC-MS | SHIMADZU EUROPA [Internet]. [cited 2023 Mar 2]. Available from: https://www.shimadzu.eu/introduction-lc-ms
47. Romson J, Emmer Å. Mass calibration options for accurate electrospray ionization mass spectrometry. Int J Mass Spectrom. 2021 Sep 1;467:116619.
48. Nguyen HP, Schug KA, Nguyen HP, Schug KA. The advantages of ESI-MS detection in conjunction with HILIC mode separations: Fundamentals and applications. J Sep Sci [Internet]. 2008 May 1 [cited 2023 Mar 2];31(9):1465–80. Available from: https://onlinelibrary.wiley.com/doi/full/10.1002/jssc.200700630
49. Nguyen HP, Schug KA, Nguyen HP, Schug KA. The advantages of ESI-MS detection in conjunction with HILIC mode separations: Fundamentals and applications. J Sep Sci [Internet]. 2008 May 1 [cited 2023 Mar 2];31(9):1465–80. Available from: https://onlinelibrary.wiley.com/doi/full/10.1002/jssc.200700630
50. Romson J, Emmer Å. Mass calibration options for accurate electrospray ionization mass spectrometry. Int J Mass Spectrom. 2021 Sep 1;467:116619.
51. Cha E, Kim S, Kim HJ, Lee KM, Kim KH, Kwon OS, et al. Sensitivity of GC-EI/MS, GC-EI/MS/MS, LC-ESI/MS/MS, LC-Ag+CIS/MS/MS, and GC-ESI/MS/MS for analysis of anabolic steroids in doping control. Drug Test Anal [Internet]. 2015 Dec 1 [cited 2023 Mar 2];7(11–12):1040–9. Available from: https://onlinelibrary.wiley.com/doi/full/10.1002/dta.1906
52. Ahamad J, Ali F, Sayed MA, Ahmad J, Nollet LML. Basic Principles and Fundamental Aspects of Mass Spectrometry. Mass Spectrometry in Food Analysis. 2022 Mar 9;3–17.
53. Valaskovic GA, Kelleher NL, Little DP, Aaserud DJ, McLafferty FW. Attomole-Sensitivity Electrospray Source for Large-Molecule Mass Spectrometry. Anal

Chem [Internet]. 1995 [cited 2023 Mar 2];67(20):3802–5. Available from: https://pubs.acs.org/doi/abs/10.1021/ac00116a030
54. Romson J, Emmer Å. Mass calibration options for accurate electrospray ionization mass spectrometry. Int J Mass Spectrom. 2021 Sep 1;467:116619.
55. Koppenaal DW, Barinaga CJ, Denton MB, Sperline RP, Hieftje GM, Schilling GD, et al. MS detectors. Anal Chem [Internet]. 2005 Nov 1 [cited 2023 Mar 2];77(21). Available from: https://pubs.acs.org/doi/abs/10.1021/ac053495p
56. Graham AWG, Ray SJ, Enke CG, Barinaga CJ, Koppenaal DW, Hieftje GM. First distance-of-flight instrument: Opening a new paradigm in mass spectrometry. J Am Soc Mass Spectrom [Internet]. 2011 Jan 20 [cited 2023 Mar 2];22(1):110–7. Available from: https://link.springer.com/article/10.1007/s13361-010-0005-8
57. Hocart CH. Mass spectrometry: An essential tool for trace identification and quantification. Comprehensive Natural Products II: Chemistry and Biology [Internet]. 2010 Mar [cited 2023 Mar 2];9:327–88. Available from: https://www.researchgate.net/publication/230700844_Mass_Spectrometry_An_Essential_Tool_for_Trace_Identification_and_Quantification
58. Principe van tandem massaspectrometrie (MS/MS) [39]. | Wetenschappelijk schema downloaden [Internet]. [cited 2023 Mar 8]. Available from: https://www.researchgate.net/figure/Principle-of-tandem-mass-spectrometry-MS-MS-39_fig4_329422876
59. Righetti L, Dreolin N, Celma A, McCullagh M, Barknowitz G, Sancho J V., et al. Travelling wave ion mobility-derived collision cross section for mycotoxins: Investigating interlaboratory and interplatform reproducibility. J Agric Food Chem [Internet]. 2020 Sep 30 [cited 2023 May 10];68(39):10937–43. Available from: https://pubs.acs.org/doi/full/10.1021/acs.jafc.0c04498
60. Righetti L, Bergmann A, Galaverna G, Rolfsson O, Paglia G, Dall'Asta C. Ion mobility-derived collision cross section database: Application to mycotoxin analysis. Anal Chim Acta. 2018 Jul 19;1014:50–7.
61. Kenderdine T, Nemati R, Baker A, Palmer M, Ujma J, FitzGibbon M, et al. High-resolution ion mobility spectrometry-mass spectrometry of isomeric/isobaric ribonucleotide variants. Journal of Mass Spectrometry. 2020 Feb 1;55(2).
62. Morris CB, Poland JC, May JC, McLean JA. Fundamentals of Ion Mobility-Mass Spectrometry for the Analysis of Biomolecules. Methods in Molecular Biology [Internet]. 2020 [cited 2023 May 8];2084:1–31. Available from: https://link.springer.com/protocol/10.1007/978-1-0716-0030-6_1
63. Screening and characterization : Waters [Internet]. [cited 2023 May 8]. Available from: https://ims.waters.com/applications-of-ims-ms/screening-and-characterization/
64. Kruve A, Rebane R, Kipper K, Oldekop ML, Evard H, Herodes K, et al. Tutorial review on validation of liquid chromatography-mass spectrometry methods: Part II. Anal Chim Acta. 2015;870(1):8–28.
65. Mei H, Hsieh Y, Nardo C, Xu X, Wang S, Ng K, et al. Investigation of matrix effects in bioanalytical high-performance liquid chromatography/tandem mass spectrometric assays: application to drug discovery. Rapid Communications in Mass Spectrometry [Internet]. 2003 Jan 15 [cited 2023 Feb 27];17(1):97–103. Available from: https://onlinelibrary.wiley.com/doi/full/10.1002/rcm.876

66. Dreolin N, Foddy H, Adams S, Hird S, Hancock P. Method Development and Validation for the Determination of Pyrrolizidine Alkaloids in a Range of Plant-Based Foods and Honey Using LC-MS/MS.
67. Shimshoni JA, Duebecke A, Mulder PPJ, Cuneah O, Barel S. Pyrrolizidine and tropane alkaloids in teas and the herbal teas peppermint, rooibos and chamomile in the Israeli market. http://dx.doi.org/101080/1944004920151087651 [Internet]. 2015 Dec 2 [cited 2023 Mar 1];32(12):2058–67. Available from: https://www.tandfonline.com/doi/abs/10.1080/19440049.2015.1087651
68. Kaczyński P, Łozowicka B. A novel approach for fast and simple determination pyrrolizidine alkaloids in herbs by ultrasound-assisted dispersive solid phase extraction method coupled to liquid chromatography–tandem mass spectrometry. J Pharm Biomed Anal. 2020 Aug 5;187:113351.
69. Bodi D, Ronczka S, Gottschalk C, Behr N, Skibba A, Wagner M, et al. Determination of pyrrolizidine alkaloids in tea, herbal drugs and honey. Food Addit Contam Part A Chem Anal Control Expo Risk Assess [Internet]. 2014 Nov 2 [cited 2023 Feb 28];31(11):1886–95. Available from: https://www.tandfonline.com/doi/abs/10.1080/19440049.2014.964337
70. Romera-Torres A, Romero-González R, Martínez Vidal JL, Garrido Frenich A. Simultaneous analysis of tropane alkaloids in teas and herbal teas by liquid chromatography coupled to high-resolution mass spectrometry (Orbitrap). J Sep Sci [Internet]. 2018 May 1 [cited 2023 Mar 6];41(9):1938–46. Available from: https://onlinelibrary.wiley.com/doi/full/10.1002/jssc.201701485
71. Bodi D, Ronczka S, Gottschalk C, Behr N, Skibba A, Wagner M, et al. Determination of pyrrolizidine alkaloids in tea, herbal drugs and honey. 2014 [cited 2023 Mar 13]; Available from: https://www.tandfonline.com/action/journalInformation?journalCode=tfac20
72. Goscinny S, McCullagh M, Far J, De Pauw E, Eppe G. Towards the use of ion mobility mass spectrometry derived collision cross section as a screening approach for unambiguous identification of targeted pesticides in food. Rapid Communications in Mass Spectrometry [Internet]. 2019 Jul 1 [cited 2023 May 11];33(S2):34–48. Available from: https://onlinelibrary.wiley.com/doi/full/10.1002/rcm.8395
73. Carbonell-Rozas L, Hernández-Mesa M, Righetti L, Monteau F, Lara FJ, Gámiz-Gracia L, et al. Ion mobility-mass spectrometry to extend analytical performance in the determination of ergot alkaloids in cereal samples. J Chromatogr A. 2022 Oct 25;1682:463502.
74. Dzuman Z, Jonatova P, Stranska-Zachariasova M, Prusova N, Brabenec O, Novakova A, et al. Development of a new LC-MS method for accurate and sensitive determination of 33 pyrrolizidine and 21 tropane alkaloids in plant-based food matrices. [cited 2023 Mar 13]; Available from: https://doi.org/10.1007/s00216-020-02848-6
75. Wu H, Fan D, Cheng J. Development and Validation of an UHPLC–MS/MS Method for the Determination of 32 Pyrrolizidine Alkaloids in Chinese Wild Honey. J AOAC Int [Internet]. 2022 Dec 22 [cited 2023 Mar 13];106(1):56–64. Available from: https://academic.oup.com/jaoac/article/106/1/56/6655681
76. Shimshoni JA, Duebecke A, Mulder PPJ, Cuneah O, Barel S. Pyrrolizidine and tropane alkaloids in teas and the herbal teas peppermint, rooibos and

chamomile in the Israeli market. http://dx.doi.org/101080/1944004920151087651 [Internet]. 2015 Dec 2 [cited 2023 Mar 1];32(12):2058–67. Available from: https://www.tandfonline.com/doi/abs/10.1080/19440049.2015.1087651
77. Crews C, Berthiller F, Krska R. Update on analytical methods for toxic pyrrolizidine alkaloids.
78. SUMMARY REPORT OF THE STANDING COMMITTEE ON PLANTS, ANIMALS, FOOD AND FEED HELD IN BRUSSELS ON 17 SEPTEMBER 2018 (Section Novel Food and Toxicological Safety of the Food Chain). [cited 2023 Apr 18]; Available from: https://circabc.europa.eu/w/browse/6b693e53-a6ac-42e5-8922-b75d2661b3cb

8. ATTATCHEMENTS

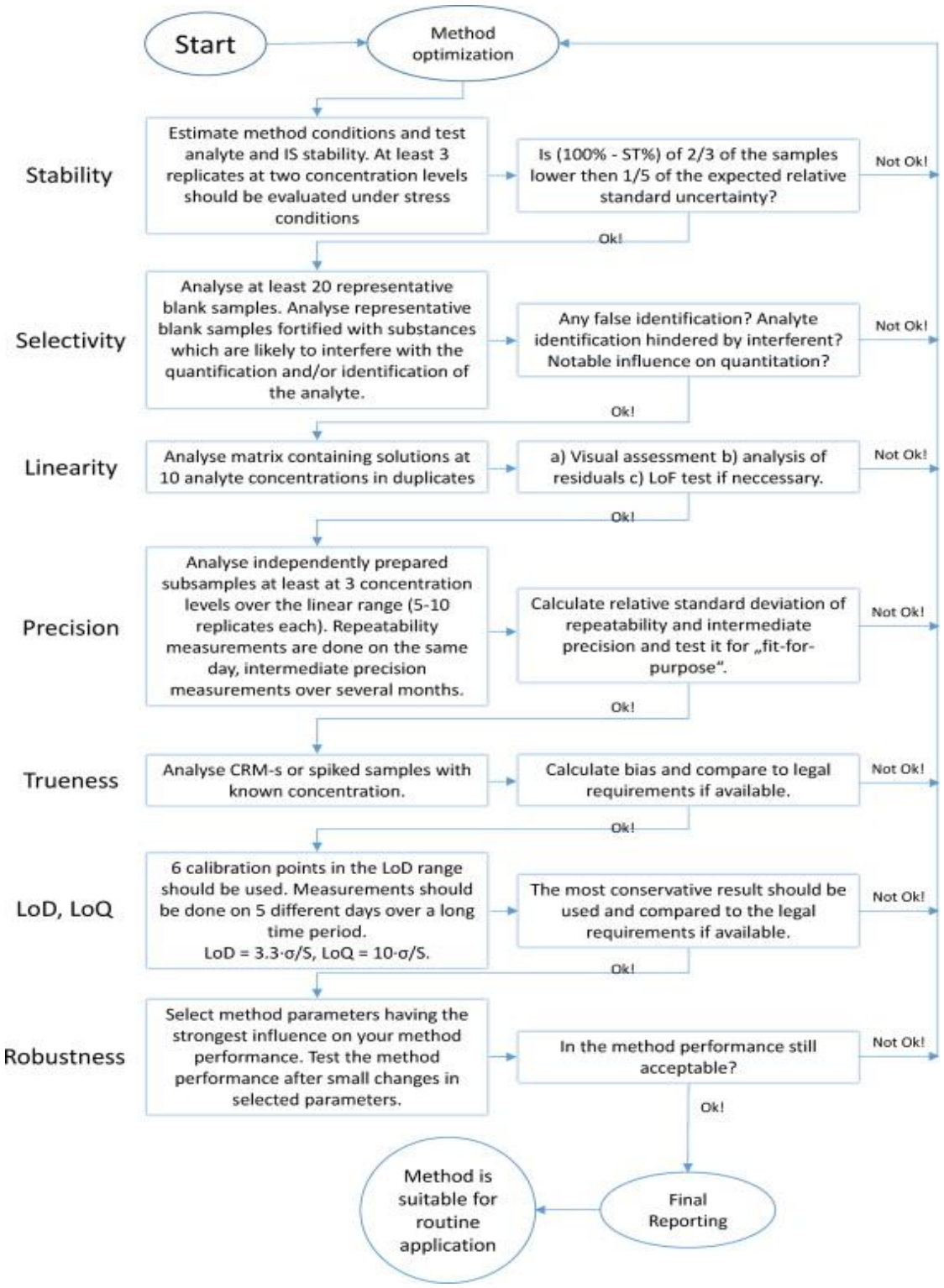

Figure 1.8 (64)

Schematic overview of a possible sequence of operations in LC-MS/MS method validation.

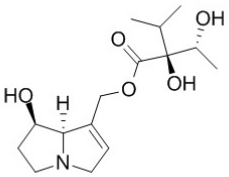

1. Intermedine

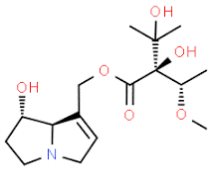

2. Europine

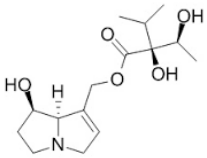

3. Lycopsamine

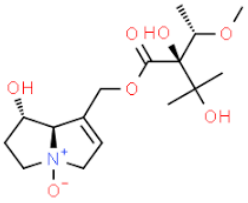

4. Europine N-oxide

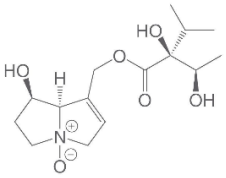

5. Intermedine N-oxide

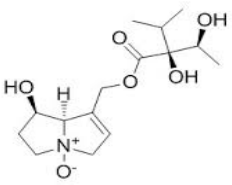

6. Lycopsamine N-oxide

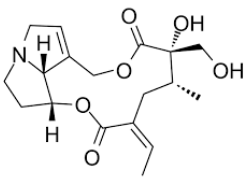

7. Retrorsine

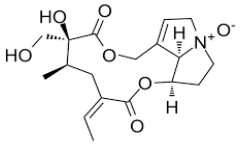

8. Retrorsine N-oxide

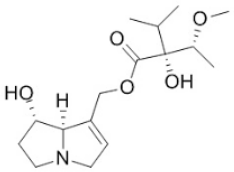

9. Heliotritine

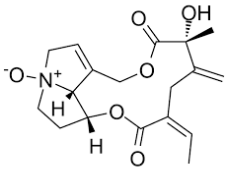

10. Seneciphylline N-oxide

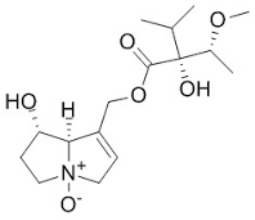

11. Heliotrine N-oxide

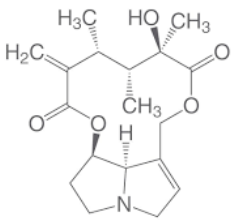

12. Senecivernine

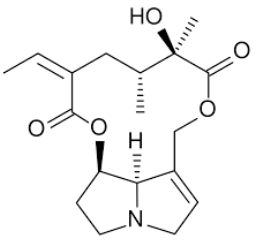

13. Senecionine

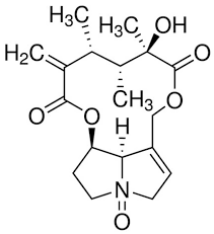

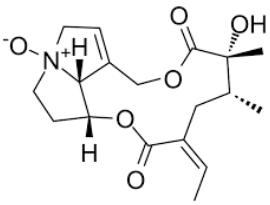

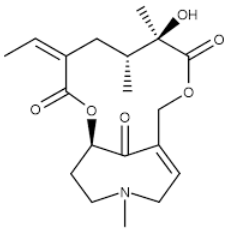

14. Senecivernine N-oxide **15.** Senecionine N-oxide **16.** Senkirkine

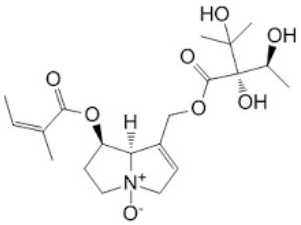
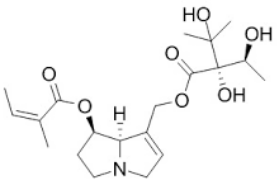
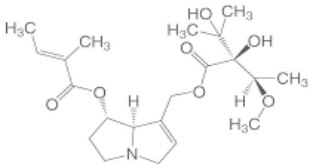

17. Echimidine N-oxide **18.** Echimidine **19.** Lasiocarpine

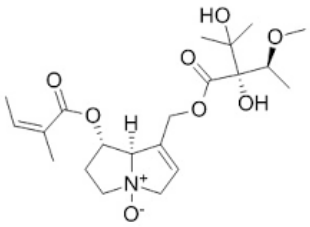
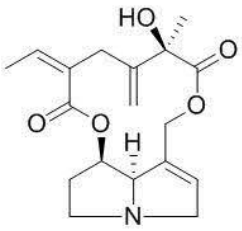

20. Lasiocarpine N-oxide **21.** Seneciphylline

Figure 2.1 (66,75)

Structural overview of the 21 investigated Pyrrolizidine alkaloids. The structure can be either mono-ester, cyclic diester, open chain diesters.

Table 3.2

Product information of the 15 screened tea samples, using a Vion IMS Mass Spectrometer.

Nº	Commercial name	Composition
1	Organic yogi Sweet dreams valerian root, rooibos	**Rooibos** (26%), mint (13%), rosemary, cinnamon, fennel, coriander, thyme, valerian root (5%), lavender flowers (3.5%), hops, aniseed (2%), vanilla.
2	Black elk, Digestive herbal tea	**Mint** (40%), chamomile (36%), fennel (24%).
3	Cupper, chamomile and peach infusion	**Chamomile** (76%), rosehip, natural peach flavor (6.5%), orange peel, natural mango flavor, natural orange flavor.

4	Conad chamomile & melissa	**Chamomile** (42%), peppermint, hawthorn, lemon balm (12%), lavender, linden.
5	Lipton mint, verbena & licorice	**Mint** (27%), chamomile, lemon verbena (15%), licorice root (9%), peppermint leaves (8.4%), rooibos, natural flavoring, lemon peel.
6	Conad fennel, mint & anise	**Fennel** (48%), ginger (30%), peppermint (12%), anise (5%), cinnamon, lavender.
7	Pompadour chamomile, fennel	Sifted **chamomile** (60%), fennel seeds (40%).
8	Lipton verbena, linden & chamomile flowers	**Lemon verbena** (56%), orange leaves (15%), natural flavoring, linden (9%), lavender (5%), chamomile (4%).
9	L'Angelica after meal mint, fennel plus mix of 5 medicinal herbs	**Mint**, licorice, melissa, fennel, lavender, caraway, cinchona, gentian.
10	Bonomelli with chamomile, lemon balm, linden and passiflora	**Chamomile** flowers (26.5%), aerial lemongrass (22%), orange leaves, sweet blackberry leaves, lemon balm leaves (10%), silver linden flowers (7.5%), natural flavoring, hawthorn flowers (3%) , passion flower aerial part (2%), mandarin peel, orange peel.
11	Pompadour melissa	**Melissa** (70%), verbena (30%).
12	Angelica fennel	**Fennel**, star anise.
13	Angelica draining otyhosiphon, fennel plus mix of 6 medicinal herbs	**Fennel**, orthosiphon, horsetail, licorice, birch, nettle, lavender, mint.
14	Vivibio fennel Infusion	**Fennel** (100%).
15	Tè verde (Conad)	**Green tea** (100%).

Table 3.3

***Overview of possible liquid-liquid extraction methods for pyrrolizidine alkaloids, found in literature* (8) (68).**

Analyte	Sample (amount)	Extraction conditions	Other treatments	Recovery %
Pyrrolizidine alkaloids + 4 tropane alkaloids	Green tea, black tea, chamomile, fennel, melissa, peppermint and rooibos (1 g)	Add (10 ml) extraction solution (aqueous acetic acid / MeOH, 1:2 v/v) Agitation (30 min) Centrifugation (10 min, 400 g)	Dilute with NH_4OH Evaporate with N_2 at 40°C Reconstituted in H_2O Filter	80-95
Pyrrolizidine alkaloids + 19 tropane alkaloids	Herbal tea (1 g)	Add (10 ml) extraction solution (MeOH/ H_2O/ formic acid, 60:39.6:0.4, v/v/v) Agitation (30 min) Centrifugation (5 min, 13.081 g)	Micro-filtering of supernatant (0.22 µm)	78-115 95-111 At 84-110 Sc

Table 3.4

Applied gradient program for sample screening with a Vion IMS QTOF Mass Spectrometer.

Time (min)	% A (Aqueous)	% B (Organic)
0.0	95	5
1.0	95	5
12.0	85	15
20.0	65	35
20.5	5	95
22.0	5	95
22.1	95	5
24.5	95	5

Table 3.5

Overview of the applied liquid-chromatography conditions, of the newly developed QqQ UPLC-MS/MS method.

Liquid-chromatography conditions	
Chromatographic system	ACQUITY™ UPLC I-Class PLUS System with column manager
Autosampler and injector	Flow Through Needle injector (FTN) with 15-µL needle
Column	ACQUITY UPLC BEH™ C8 (2.1 × 100 mm, 1.7 µm particle size, 130 Å pore size, p/n: 186002878)
Aqueous mobile phase	2 mM ammonium formate in water + 0.2% formic acid (v/v%)
Organic mobile phase	2 mM ammonium formate in methanol + 0.2% formic acid (v/v%)
Needle wash solvent	Water : methanol : acetonitrile : isopropanol (20:40:20:20 + 0.5% formic acid volumetrically)
Seal wash solvent	Water : methanol (80:20, v/v%)

Table 3.6

Overview of the tested gradients of all eight different methods. Method 8 is the chosen gradient, for the new QqQ method.

Method	Time (min)	% A (Aqueous)	% B (Organic)
1			
	0	95	5
	1.0	95	5
	12.0	85	15
	20.0	65	35
	20.5	5	95
	22.0	5	95
	22.1	95	5
	30.0	95	5
2			
	0.0	90	10
	8.0	70	30
	16.0	40	60
	17.0	0	100
	19.0	0	100
	20.0	90	10
	25.0	90	10
3			
	0.0	98	2
	8.0	70	30
	16.0	40	60
	17.0	0	100
	19.0	0	100
	20.0	90	10
	25.0	90	10
4			
	0.0	90	10
	2.0	70	30
	16.0	40	60
	17.0	0	100
	19.0	0	100
	20.0	90	10
	25.0	90	10
5			
	0.0	100	0
	5.0	70	30
	15.0	40	60
	16.0	0	100
	18.0	0	100
	19.0	90	10
	25.0	90	10
6			
	0.0	100	0
	2.0	90	10
	3.0	90	10
	5.0	80	20

	6.0	60	40
	15.0	40	60
	16.0	0	100
	18.0	0	100
	19.0	100	0
	25.0	100	0
7			
	0.0	100	0
	1.0	90	10
	2.0	90	10
	6.0	80	20
	7.0	60	40
	15.0	40	60
	16.0	0	100
	18.0	0	100
	19.0	100	0
	25.0	100	0
8			
	0.0	100	0
	1.0	90	10
	2.0	90	10
	6.0	80	20
	7.0	60	40
	13.0	50	50
	15.0	40	60
	16.0	0	100
	18.0	0	100
	19.0	100	0
	25.0	100	0

Table 3.7

Overview of the applied mass-spectrometry conditions, of the newly developed QqQ UPLC-MS/MS method.

MS/MS conditions	
MS system	Xevo TQ-S micro
Ionization mode	ESI+
Acquisition mode	Multiple Reaction Monitoring (MRM)
Capillary voltage	+ 0.75 kV
Cone gas flow	50 L/Hr

Desolvation temperature	600°C
Desolvation gas flow	850 L/Hr
Source temperature	150°C
Resolution	MS1 Unit, MS2 Unit
Software	waters_connect™ for quantitation (v. 1.0.) for data acquisition and processing

Table 3.8

MS information of the standard solution containing 21 PAs. The mixture is analyzed, using the chosen UPLC-MS/MS parameters of the new QqQ method. RT, molecular formula, precursor and product ion, and collision energy are displayed, for each of the 21 PAs.

Analyte	RT (min)	Molecular formula	Precursor ion (*m/z*)	Product ion (*m/z*)	Collision energy (eV)
1 Intermedine	6.68	$C_{15}H_{25}NO_5$	300.2	94.0 138.1	25
2 Europine	6.95	$C_{16}H_{27}NO_6$	330.2	138.0 156.0	20
3 Lycopsamine	6.96	$C_{15}H_{25}NO_5$	300.2	94.0 156.1	25
4 Europine N-oxide	7.52	$C_{16}H_{27}NO_7$	346.2	172.0 111.0	30
5 Intermedine N-oxide	7.80	$C_{15}H_{25}NO_6$	316.2	172.0 94.0	26
6 Lycopsamine N-oxide	8.08	$C_{15}H_{25}NO_6$	316.2	172.0 94.0	26
7 Retrorsine	8.70	$C_{18}H_{25}NO_6$	352.2	120.1 94.0	28
8 Retrorsine N-oxide	8.93	$C_{18}H_{25}NO_7$	368.2	94.0 120.1	47
9 Seneciphylline	9.22	$C_{18}H_{23}NO_5$	334.2	94.0 120.1	34
10 Heliotrine	9.49	$C_{16}H_{27}NO_5$	314.2	138.0 156.0	20
11 Heliotrine N-oxide	9.92	$C_{16}H_{27}NO_6$	330.2	172.0 111.0	26

12 Seneciphylline N-oxide	9.65	$C_{18}H_{23}NO_6$	350.2	94.0 120.0	42
13 Senecivernine	10.22	$C_{18}H_{25}NO_5$	336.2	120.1 81.1	28
14 Senecionine	10.22	$C_{18}H_{25}NO_5$	336.2	94.0 120.1	32
15 Senecivernine N-oxide	10.36	$C_{18}H_{25}NO_6$	352.2	94.0 120.0	45
16 Senecionine N-oxide	10.58	$C_{18}H_{25}NO_6$	352.2	118.0 94.0	30
17 Senkirkine	11.21	$C_{19}H_{27}NO_6$	366.2	122.0 168.1	32
18 Echimidine N-oxide	11.08	$C_{20}H_{31}NO_8$	414.2	254.1 83.0	30
19 Echimidine	11.22	$C_{20}H_{31}NO_7$	398.2	120.0 83.0	25
20 lasiocarpine	11.26	$C_{21}H_{33}NO_7$	421.2	120.0 220.0	28
21 Lasiocarpine N-oxide	12.76	$C_{21}H_{33}NO_8$	428.2	94.0 254.1	48

Table 4.1

***Overview of possible solid-liquid extraction (SLE) methods and supplementary clean-up to extract pyrrolizidine alkaloids. This information was pooled from different sources* (26,28,69)**

Analyte	Sample (amount)	Extraction Conditions	SPE clean-up
Pyrrolizidine alkaloids	Samples (250 g) Tea bags (3 packages from the same lot)	- Homogenize - Ultra-centrifugal mill => particle size < 0.5 mm - Avoid heating => (1:3 ratio) dry ice: sample - Ultra-centrifugal mill (1200 min^{-1}) - 2 g Sample in 50 mL polypropylene centrifuge + 40 mL 2% (v/v) formic acid in water - Vortex briefly vertical shaker (30 min, 20°C)	- Macherey-Nagel HR-X cartridges (60 mg, 30 mL) for the Gerstel MultiPurpose sampler®. - Cartridges conditioning: 5 mL methanol + 5 mL H_2O - 5 mL sample extract transferred onto cartridge - Wash whit 5 mL H_2O - Dry cartridge (3 min, nitrogen stream) - Elution: 5 mL methanol in glass test-tube - Evaporate solvent (40°C, ambient nitrogen stream)

		- Centrifuge (15 min, 3600 min^{-1}) - 5 mL Supernatants in 15 mL polypropylene centrifuge tube - pH 10 by 25% ammonia - Shake (15 min) + centrifuge (3600 min^{-1})	- Reconstitute sample 500 µl water/methanol (1:9, v/v%) - Transfer in filtered vial (cellulose, 0.2 µm) - UPLC-MS/MS analysis
Pyrrolizidine alkaloids	Commercial tea samples (2 g): lemon balm, fennel tea, hibiscus, chrysanthemum, lavender, chamomile, rooibos, peppermint, mix tea, black and green tea	- Homogenize - Sample (2 g) in 50 mL graduated polyethylene tube - Extraction (30 min) + shaking with 40 mL 0.05 M sulfuric acid in 50% methanol solution - Centrifuge (10 min, 2900 G) - Supernatants into (50-mL) tube and passed through fluted filter paper	- Condition SPE cartridge: 3 mL methanol + 3 mL H_2O - Filtered crude extract (2 mL) passed through SPE cartridge (2 mL/min) - Wash with 4 mL H_2O - Elute with 4 mL of 2.5% ammonia in methanol - Dry cartridge (nitrogen gas) - Dissolve (1 mL of 5% methanol) - Filter the solution trough a 0.22 µm PTFE chromacol syringe filter - LC-MS/MS analysis
Pyrrolizidine alkaloids	Commercial tea samples: peppermint, chamomile, fennel, anise, caraway, melissa and nettle	- Homogenize - Mix with dry ice (mass ratio 2:1) - Stir for 3 min - Ultra-centrifugal mill=> particle size < 500 µm - Ultra sonication (15 min) => 2 g sample extracted with 20 mL aqueous sulphuric acid solution (0.05 M) - Supernatants decanted - Repeat the extraction - Combine supernatants pH 6-7 with diluted ammonia solution - Passe through fluted filter paper	- Conditioning reversed phase C18 SPE cartridges (Discovery DSC-C18 500 mg/6 mL) with 5 mL methanol+ 5 mL H_2O - Loading of the cartridges with 10 mL sample extract - Wash with 6 mL H_2O - Dry (using vacuum manifold 5-10 min) - Elution: 5 mL methanol OR 2.5% (1.4 M) ammonia in methanol (for black and green tea) - Dried in a heated (50°C) water bath under a nitrogen stream - Reconstitution: 1 mL methanol: water (5:95 v/v%) - Reconstituted samples filtered trough (Nylon, 0.2 µm, at 13 000 g)

Table 4.5

35 Eu-regulated PA standards were injected in two different concentrations into the Vion IMS QTOF analyser. This table provides a summary of all the obtained paramters. Neutral mass, observed neutral mass, observed m/z, mass error, observed drift and the observed CCS for each PA.

Component name	Neutral mass (Da)	Observed neutral mass (Da)	Observed *m/z*	Mass error (mDa)	Observed drift (ms)	Observed CCS (Å²)	dilution
Echimidine	397.21005	397.2097	398.2170	-0.4	4.36	193.69	200
Echimidine	397.21005	397.2098	398.2171	-0.2	4.35	193.37	200
Echimidine	397.21005	397.2100	398.2172	-0.1	4.33	192.71	20
Echimidine-N-oxide	413.20497	413.2046	414.2119	-0.3	4.39	194.20	200
Echimidine-N-oxide	413.20497	413.2046	414.2119	-0.3	4.39	194.20	200
Echimidine-N-oxide	413.20497	413.2046	414.2119	-0.3	4.39	194.20	20
Echinatine	299.17327	299.1729	300.1802	-0.4	3.41	169.60	200
Echinatine	299.17327	299.1730	300.1803	-0.3	3.42	169.68	200
Echinatine	299.17327	299.1730	300.1803	-0.3	3.42	169.68	20
Echinatine-N-oxide	315.16819	315.1677	316.1750	-0.4	3.38	168.60	200
Echinatine-N-oxide	315.16819	315.1677	316.1750	-0.4	3.38	168.60	200
Echinatine-N-oxide	315.16819	315.1677	316.1750	-0.4	3.38	168.60	20
Europine	329.18384	329.1836	330.1908	-0.3	3.68	176.07	200
Europine	329.18384	329.1836	330.1908	-0.3	3.68	176.07	200
Europine	329.18384	329.1836	330.1908	-0.3	3.68	176.07	20
Europine-N-oxide	345.17875	345.1786	346.1859	-0.2	3.60	173.75	200
Europine-N-oxide	345.17875	345.1786	346.1859	-0.2	3.60	173.75	200
Europine-N-oxide	345.17875	345.1786	346.1859	-0.2	3.60	173.75	20
Heliosupine	397.21005	397.2100	398.2173	0	4.30	192.06	200
Heliosupine	397.21005	397.2100	398.2173	0	4.30	192.06	200
Heliosupine	397.21005	397.2100	398.2173	0	4.30	192.06	20
Heliosupine-N-oxide	413.20497	413.2045	414.2118	-0.4	4.24	190.17	200
Heliosupine-N-oxide	413.20497	413.2045	414.2118	-0.4	4.24	190.17	200
Heliosupine-N-oxide	413.20497	413.2045	414.2118	-0.4	4.24	190.17	20
Heliotrine	313.18892	313.1886	314.1959	-0.3	3.60	174.17	200
Heliotrine	313.18892	313.1886	314.1959	-0.3	3.61	174.45	200
Heliotrine	313.18892	313.1888	314.1961	-0.1	3.58	173.57	20
Heliotrine-N-oxide	329.18384	329.1835	330.1908	-0.3	3.56	172.84	200
Heliotrine-N-oxide	329.18384	329.1837	330.1910	-0.1	3.55	172.82	200
Heliotrine-N-oxide	329.18384	329.1839	330.1912	0.1	3.54	172.53	20
Indicine	299.17327	299.1729	300.1801	-0.4	3.48	171.18	200

Indicine	299.17327	299.1730	300.1803	-0.3	3.47	170.96	200
Indicine	299.17327	299.1733	300.1806	0.1	3.45	170.44	20
Indicine-N-oxide	315.16819	315.1682	316.1755	0	3.46	170.47	200
Indicine-N-oxide	315.16819	315.1678	316.1751	-0.4	3.41	169.37	200
Indicine-N-oxide	315.16819	315.1684	316.1757	0.2	3.44	169.92	20
Integerrimine	335.17327	335.1729	336.1802	-0.4	3.80	179.24	200
Integerrimine	335.17327	335.1728	336.1800	-0.5	3.80	179.08	200
Integerrimine	335.17327	335.1734	336.1807	0.1	3.77	178.25	20
Integerrimine-N-oxide	351.16819	351.1678	352.1751	-0.4	3.83	179.69	200
Integerrimine-N-oxide	351.16819	351.1681	352.1754	-0.1	3.83	179.85	200
Integerrimine-N-oxide	351.16819	351.1680	352.1753	-0.2	3.84	179.95	20
Intermedine	299.17327	299.1733	300.1805	0	3.43	169.98	200
Intermedine	299.17327	299.1735	300.1808	0.3	3.41	169.56	200
Intermedine	299.17327	299.1729	300.1802	-0.4	3.44	170.24	20
Intermedine-N-oxide	315.16819	315.1680	316.1753	-0.1	3.42	169.59	200
Intermedine-N-oxide	315.16819	315.1682	316.1755	0	3.44	169.92	200
Intermedine-N-oxide	315.16819	315.1682	316.1755	0	3.45	170.31	20
Lasiocarpine	411.2257	411.2256	412.2329	-0.1	4.51	197.63	200
Lasiocarpine	411.2257	411.2254	412.2327	-0.3	4.47	196.59	200
Lasiocarpine	411.2257	411.2254	412.2327	-0.3	4.47	196.59	20
Lasiocarpine-N-oxide	427.2062	427.2205	428.2277	-0.2	4.42	194.96	200
Lasiocarpine-N-oxide	427.22062	427.2205	428.2278	-0.1	4.41	194.79	200
Lasiocarpine-N-oxide	427.22062	427.2206	428.2279	0	4.41	194.90	20
Lycopsamine	299.17327	299.1732	300.1804	-0.1	3.42	169.85	200
Lycopsamine	299.17327	299.1729	300.1802	-0.4	3.39	168.90	200
Lycopsamine	299.17327	299.1735	300.1808	0.3	3.40	169.31	20
Lycopsamine-N-oxide	315.16819	315.1678	316.1751	-0.4	3.36	168.05	200
Lycopsamine-N-oxide	315.16819	315.1680	316.1752	-0.2	3.35	167.81	200
Lycopsamine-N-oxide	315.16819	315.1679	316.1751	-0.3	3.35	167.67	20
Retrorsine	351.16819	351.1675	352.1748	-0.6	3.88	181.00	200
Retrorsine	351.16819	351.1677	352.1750	-0.5	3.88	181.21	200
Retrorsine	351.16819	351.1682	352.1754	0	3.85	180.23	20
Retrorsine-N-oxide	367.1631	367.1625	368.1698	-0.6	3.92	181.89	200
Retrorsine-N-oxide	367.1631	367.1628	368.1701	-0.3	3.95	182.82	200
Retrorsine-N-oxide	367.1631	367.1627	368.1699	-0.4	3.90	181.54	20
Rinderine	299.17327	299.1732	300.1805	0	3.44	170.15	200
Rinderine	299.17327	299.1729	300.1802	-0.4	3.42	169.84	200
Rinderine	299.17327	299.1733	300.1806	0.1	3.40	169.12	20
Rinderine-N-oxide	315.16819	315.1679	316.1752	-0.2	3.43	169.70	200
Rinderine-N-oxide	315.16819	315.1681	316.1754	-0.1	3.43	169.75	200

Rinderine-N-oxide	315.16819	315.1679	316.1752	-0.3	3.42	169.42	20
Senecionine	335.17327	335.1729	336.1802	-0.4	3.79	178.81	200
Senecionine	335.17327	335.1729	336.1801	-0.4	3.78	178.72	200
Senecionine	335.17327	335.1731	336.1804	-0.2	3.75	177.97	20
Senecionine-N-oxide	351.16819	351.1675	352.1748	-0.7	3.84	179.98	200
Senecionine-N-oxide	351.16819	351.1678	352.1751	-0.4	3.84	180.01	200
Senecionine-N-oxide	351.16819	351.1680	352.1752	-0.2	3.80	179.05	20
Seneciphylline	333.15762	333.1571	334.1644	-0.5	3.68	176.16	200
Seneciphylline	333.15762	333.1570	334.1643	-0.6	3.69	176.43	200
Seneciphylline	333.15762	333.1574	334.1647	-0.2	3.67	175.86	20
Seneciphylline-N-oxide	349.15254	349.1521	350.1594	-0.4	3.74	177.54	200
Seneciphylline-N-oxide	349.15254	349.1525	350.1598	-0.1	3.75	177.58	200
Seneciphylline-N-oxide	349.15254	349.1524	350.1597	-0.1	3.72	176.95	20
Senecivernine	335.17327	335.1730	336.1803	-0.3	3.77	178.26	200
Senecivernine	335.17327	335.1728	336.1800	-0.5	3.76	178.14	200
Senecivernine	335.17327	335.1731	336.1804	-0.2	3.71	176.86	20
Senecivernine-N-oxide	351.16819	351.1679	352.1752	-0.2	3.81	179.35	200
Senecivernine-N-oxide	351.16819	351.1679	352.1752	-0.3	3.82	179.48	200
Senecivernine-N-oxide	351.16819	351.1680	352.1753	-0.2	3.78	178.48	20
Senkirkine	365.18384	365.1838	366.1910	-0.1	3.85	180.23	200
Senkirkine	365.18384	365.1836	366.1909	-0.3	3.86	180.40	200
Senkirkine	365.18384	365.1838	366.1911	0	3.86	180.32	20
Spartioidine	333.15762	333.1572	334.1644	-0.5	3.72	177.00	200
Spartioidine	333.15762	333.1574	334.1647	-0.2	3.72	177.02	200
Spartioidine	333.15762	333.1578	334.1650	0.1	3.69	176.37	20
Spartioidine-N-oxide	349.15254	349.1523	350.1596	-0.2	3.78	178.58	200
Spartioidine-N-oxide	349.15254	349.1522	350.1595	-0.3	3.78	178.58	200
Spartioidine-N-oxide	349.15254	349.1525	350.1597	-0.1	3.75	177.66	20
Usaramine	351.16819	351.1677	352.1750	-0.5	3.88	181.10	200
Usaramine	351.16819	351.1679	352.1752	-0.3	3.90	181.53	200
Usaramine	351.16819	351.1682	352.1755	0	3.84	180.05	20
Usaramine-N-oxide	367.1631	367.1629	368.1702	-0.2	3.93	182.34	200
Usaramine-N-oxide	367.1631	367.1627	368.1700	-0.4	3.95	182.75	200
Usaramine-N-oxide	367.1631	367.1628	368.1701	-0.3	3.91	181.88	20

Table 4.6

Summary table: CCS values predicted by two machine-learning algorithems (AllCCS and CCSbase), based on the SMILE string of each PA. The CCS was predicted for multiple adducts. Mean observed CCS values, were calculeted from Table 4.5 above. A prediction error for both algorithems was calculated for the most abundant ion $[M+H]^+$.

Name	SMILE	Adduct	*m/z*	Predicted CCS (*AllCCS*)	Predicted CCS (*CCSbase*)	Observed CCS	Prediction error % (AllCCS)	Prediction error % (*CCSbase*)
Intermedine	CC(C)C(C(C)O)(C(=O)OCC1=CCN2C1C(CC2)O)O	[M+H]+	300.18	169.9	175.1	169.93	0.06	3.00
		[M+H-H2O]+	282.17	166.8	/			
		[M+Na]+	322.16	173.5	177.5			
		[M+NH4]+	317.21	172.7	176.4			
		[M-H]-	298.17	173.4	176.7			
		[M+Na-2H]-	320.15	173.7	174.7			
		[M+HCOO]-	344.17	174.2	/			
Europine	CC(C(C(=O)OCC1=CCN2C1C(CC2)O)(C(C)(C)O)O)OC	[M+H]+	330.19	176.6	185.1	176.07	0.30	5.13
		[M+H-H2O]+	312.18	173.8	/			
		[M+Na]+	352.17	179.9	189.6			
		[M+NH4]+	347.21	179.2	186.2			
		[M-H]-	328.18	180.6	187.6			
		[M+Na-2H]-	350.16	181.1	186.0			
		[M+HCOO]-	374.18	181.8	/			
Lycopsamine	C[C@@H](C[C@@](C(C)C)(C(=O)OCC1=CCN2[C@H]1[C@@H](CC2)O)O)O	[M+H]+	300.18	169.9	175.1	169.35	0.53	3.61
		[M+H-H2O]+	282.17	166.8	/			
		[M+Na]+	322.16	173.5	177.5			
		[M+NH4]+	317.21	172.7	176.4			
		[M-H]-	298.17	173.4	176.7			
		[M+Na-2H]-	320.15	173.7	174.7			
		[M+HCOO]-	344.17	174.2	/			
Europine N-oxide	CC(C(C(=O)OCC1=CC[N+]2(C1C(CC2)O)[O-])(C(C)(C)O)O)OC	[M+H]+	346.19	178.8	183.2	173.75	2.75	5.29
		[M+H-H2O]+	328.18	176.1	/			
		[M+Na]+	368.17	181.9	188.5			
		[M+NH4]+	363.21	181.2	185.8			
		[M-H]-	344.17	185.8	189.8			
		[M+Na-2H]-	366.15	186.5	198.3			
		[M+HCOO]-	390.18	187.4	/			
Intermedine N-oxide	C[C@H]([C@@](C(C)C)(C(=O)OCC1=CC[N+]2([C@H]1[C@@H](CC2)O)[O-])O)O	[M+H]+	316.18	172.2	173.9	169.94	1.29	2.29
		[M+H-H2O]+	298.16	169.3	/			
		[M+Na]+	338.16	175.6	178.3			
		[M+NH4]+	333.20	174.9	177.0			
		[M-H]-	314.16	179.2	179.9			
		[M+Na-2H]-	336.14	179.8	186.5			
		[M+HCOO]-	360.17	180.6	/			
Lycopsamine N-oxide	CC(C)C(C(C)O)(C(=O)OCC1=CC[N+]2(C1C(CC2)O)[O-])O	[M+H]+	316.18	172.2	173.9	167.84	2.5	3.51
		[M+H-H2O]+	298.16	169.3	/			
		[M+Na]+	338.16	175.6	178.3			
		[M+NH4]+	333.20	174.9	177.0			
		[M-H]-	314.16	179.2	179.9			
		[M+Na-2H]-	336.14	179.8	186.5			
		[M+HCOO]-	360.17	180.6	/			
Retrorsine	CC=C1CC(C(C(=O)OCC2=CCN3C2C(CC3)O	[M+H]+	352.18	181.9	178.9	180.81	0.50	1.16
		[M+H-H2O]+	334.16	179.0	/			
		[M+Na]+	374.16	185.4	182.0			
		[M+NH4]+	369.20	184.6	188.6			

	C1=O)(CO)O)C	[M-H]-	350.16	183.4	179.2			
		[M+Na-2H]-	372.14	183.6	172.9			
		[M+HCOO]-	396.17	183.9	/			
Retrorsine N-oxide	CC=C1CC(C(C(=O)OCC2=CC[N+]3(C2C(CC3)OC1=O)[O-])(CO)O)C	[M+H]+	368.17	184.4	182.9	182.08	1.31	0.49
		[M+H-H2O]+	350.16	181.7	/			
		[M+Na]+	390.15	187.7	179.6			
		[M+NH4]+	385.20	187.0	189.9			
		[M-H]-	366.16	188.0	181.6			
		[M+Na-2H]-	388.14	188.5	181.4			
		[M+HCOO]-	412.16	189.2	/			
Seneciphylline	CC=C1CC(=C)C(C(=O)OCC2=CCN3C2C(CC3)OC1=O)(C)O	[M+H]+	334.16	178.0	175.8	176.15	1.14	0.11
		[M+H-H2O]+	316.15	174.8	/			
		[M+Na]+	356.15	181.7	181.3			
		[M+NH4]+	351.19	180.8	186.1			
		[M-H]-	332.15	181.1	175.9			
		[M+Na-2H]-	354.13	181.0	169.5			
		[M+HCOO]-	378.16	181.2	/			
Heliotrine	CC(C)C(C(C)OC)(C(=O)OCC1=CCN2C1C(CC2)O)O	[M+H]+	314.20	174.1	178.3	174.06	0.06	2.47
		[M+H-H2O]+	296.19	171.1	/			
		[M+Na]+	336.18	177.5	181.1			
		[M+NH4]+	331.22	176.8	179.5			
		[M-H]-	312.18	177.7	180.2			
		[M+Na-2H]-	334.16	178.2	178.5			
		[M+HCOO]-	358.19	178.9	/			
Heliotrine N-oxide	C[C@H]([C@@](C(C)C)(C(=O)OCC1=CC[N+]2([C@H]1[C@H](CC2)O)[O-])O)OC	[M+H]+	330.19	176.4	177.7	172.73	1.97	2.72
		[M+H-H2O]+	312.18	173.6	/			
		[M+Na]+	352.17	179.7	182.1			
		[M+NH4]+	347.22	178.9	180.7			
		[M-H]-	328.18	183.1	184.2			
		[M+Na-2H]-	350.16	183.9	190.0			
		[M+HCOO]-	374.18	184.8	/			
Seneciphylline N-oxide	CC=C1CC(=C)C(C(=O)OCC2=CC[N+]3(C2C(CC3)OC1=O)[O-])(C)O	[M+H]+	350.16	181.2	177.9	177.36	2.37	0.51
		[M+H-H2O]+	332.15	178.3	/			
		[M+Na]+	372.14	184.7	176.5			
		[M+NH4]+	367.19	183.9	185.5			
		[M-H]-	348.15	185.5	176.3			
		[M+Na-2H]-	370.13	186.0	177.2			
		[M+HCOO]-	394.15	186.6	/			
Senecivernine	CC1C(C(C(=O)OCC2=CCN3C2C(CC3)OC(=O)C1=C)(C)O)C	[M+H]+	336.18	177.8	176.1	177.75	0.11	1.07
		[M+H-H2O]+	318.17	174.7	/			
		[M+Na]+	358.16	181.4	181.7			
		[M+NH4]+	353.21	180.6	187.0			
		[M-H]-	334.17	182.1	176.9			
		[M+Na-2H]-	356.15	182.2	170.3			
		[M+HCOO]-	380.17	182.5	/			
Senecionine	CC=C1CC(C(C(=O)OCC2=CCN3C2C(CC3)OC1=O)(C)O)C	[M+H]+	336.18	178.6	176.8	178.50	0.22	1.23
		[M+H-H2O]+	318.17	175.5	/			
		[M+Na]+	358.16	182.3	182.4			
		[M+NH4]+	353.21	181.4	187.2			
		[M-H]-	334.17	182.1	177.5			
		[M+Na-2H]-	356.15	182.2	169.9			
		[M+HCOO]-	380.17	182.5	/			
Senecivernine N-oxide	CC1C(C(C(=O)OCC2=CC[N+]3(C2C(CC3)OC(=O)C1=C)[O-])(C)O)C	[M+H]+	352.18	180.8	178.0	179.10	1.01	0.56
		[M+H-H2O]+	334.16	178.0	/			
		[M+Na]+	374.16	184.2	176.7			
		[M+NH4]+	369.20	183.5	186.1			
		[M-H]-	350.16	186.5	177.0			
		[M+Na-2H]-	372.14	187.1	177.9			
		[M+HCOO]-	396.17	187.8	/			
Senecionine N-oxide	CC=C1CC(C(C(=O)OCC2=CC[N+]	[M+H]+	352.18	181.9	178.9	179.68	1.06	0.61
		[M+H-H2O]+	334.16	179.0	/			
		[M+Na]+	374.16	185.3	177.6			

	3(C2C(CC3)OC1=O)[O-])(C)O)C	[M+NH4]+	369.20	184.5	186.6			
		[M-H]-	350.16	186.4	177.8			
		[M+Na-2H]-	372.14	187.0	177.7			
		[M+HCOO]-	396.17	187.7	/			
Senkirkine	CC=C1CC(C(C(=O)OCC2=CCN(CCC(C2=O)OC1=O)C)(C)O)C	[M+H]+	366.19	185.9	170.5	180.32	3.28	5.28
		[M+H-H2O]+	348.18	183.0	/			
		[M+Na]+	388.17	189.3	174.6			
		[M+NH4]+	383.22	188.5	176.7			
		[M-H]-	364.18	188.1	174.5			
		[M+Na-2H]-	386.16	188.7	192.9			
		[M+HCOO]-	410.19	189.5	/			
Echimidine N-oxide	CC=C(C)C(=O)OC1CC[N+]2(C1C(=CC2)COC(=O)C(C(C)O)(C(C)(C)O)O)[O-]	[M+H]+	414.21	195.8	198.3	194.20	0.82	2.11
		[M+H-H2O]+	396.20	193.7	/			
		[M+Na]+	436.19	198.3	204.1			
		[M+NH4]+	431.23	197.8	200.3			
		[M-H]-	412.20	198.9	207.4			
		[M+Na-2H]-	434.18	200.1	210.7			
		[M+HCOO]-	458.20	201.5	/			
Echimidine	CC=C(C)C(=O)OC1CCN2C1C(=CC2)COC(=O)C(C(C)O)(C(C)(C)O)O	[M+H]+	398.22	193.9	199.0	193.26	0.33	2.97
		[M+H-H2O]+	380.21	191.7	/			
		[M+Na]+	420.20	196.5	206.0			
		[M+NH4]+	415.24	196.0	201.0			
		[M-H]-	396.20	194.4	205.5			
		[M+Na-2H]-	418.18	195.4	198.6			
		[M+HCOO]-	442.21	196.6	/			
Lasiocarpine	CC=C(C)C(=O)OC1CCN2C1C(=CC2)COC(=O)C(C(C)OC)(C(C)(C)O)O	[M+H]+	412.23	198.0	203.2	196.94	0.54	3.18
		[M+H-H2O]+	394.22	195.9	/			
		[M+Na]+	434.22	200.5	209.6			
		[M+NH4]+	429.26	199.9	204.2			
		[M-H]-	410.22	198.3	208.9			
		[M+Na-2H]-	432.20	199.5	202.4			
		[M+HCOO]-	456.22	201.1	/			
Lasiocarpine N-oxide	CC=C(C)C(=O)OC1CC[N+]2(C1C(=CC2)COC(=O)C(C(C)OC)(C(C)(C)O)O)[O-]	[M+H]+	428.23	199.9	201.9	194.88	2.58	3.60
		[M+H-H2O]+	410.22	197.9	/			
		[M+Na]+	450.21	202.2	207.6			
		[M+NH4]+	445.25	201.7	203.7			
		[M-H]-	426.21	202.6	211.2			
		[M+Na-2H]-	448.20	204.0	213.9			
		[M+HCOO]-	472.22	205.6	/			

Indicine	C[C@@H]([C@](C(C)C)(C(=O)OCC1=CCN2[C@H]1[C@@H](CC2)O)O)O	[M+H]+	300.1806	169.9	175.1	170.86	0.56	2.48
		[M+H-H2O]+	282.1700	166.8	/			
		[M+Na]+	322.1626	173.5	177.5			
		[M+NH4]+	317.2072	172.7	176.4			
		[M-H]-	298.1660	173.4	176.7			
		[M+Na-2H]-	320.1480	173.7	174.7			
		[M+HCOO]-	344.1715	174.2	/			
Echinatine	CC(C)C(C(C)O)(C(=O)OCC1=CCN2C1C(CC2)O)O	[M+H]+	300.1806	169.9	175.1	169.65	0.15	3.21
		[M+H-H2O]+	282.1700	166.8	/			
		[M+Na]+	322.1626	173.5	177.5			
		[M+NH4]+	317.2072	172.7	176.4			
		[M-H]-	298.1660	173.4	176.7			
		[M+Na-2H]-	320.1480	173.7	174.7			
		[M+HCOO]-	344.1715	174.2	/			
Rinderine	C[C@H]([C@](C(C)C)(C(=O)OCC1=CCN2[C@H]1[C@H](CC2)O)O)O	[M+H]+	300.1806	169.9	175.1	169.70	0.12	3.18
		[M+H-H2O]+	282.1700	166.8	/			
		[M+Na]+	322.1626	173.5	177.5			
		[M+NH4]+	317.2072	172.7	176.4			
		[M-H]-	298.1660	173.4	176.7			
		[M+Na-2H]-	320.1480	173.7	174.7			
		[M+HCOO]-	344.1715	174.2	/			

Rinderine N-oxide	C[C@H]([C@@](C(C)C)(C(=O)OCC1=CC[N+]2([C@H]1[C@H](CC2)O)[O-])O)O	[M+H]+	316.1755	172.2	173.9	169.62	1.52	2.52
		[M+H-H2O]+	298.1649	169.3	/			
		[M+Na]+	338.1575	175.6	178.3			
		[M+NH4]+	333.2021	174.9	177.0			
		[M-H]-	314.1609	179.2	179.9			
		[M+Na-2H]-	336.1429	179.8	186.5			
		[M+HCOO]-	360.1664	180.6	/			
Echinatine N-oxide	CC(C)C(C(C)O)(C(=O)OCC1=CC[N+]2(C1C(CC2)O)[O-])O	[M+H]+	316.1755	172.2	173.9	168.60	2.14	3.14
		[M+H-H2O]+	298.1649	169.3	/			
		[M+Na]+	338.1575	175.6	178.3			
		[M+NH4]+	333.2021	174.9	177.0			
		[M-H]-	314.1609	179.2	179.9			
		[M+Na-2H]-	336.1429	179.8	186.5			
		[M+HCOO]-	360.1664	180.6	/			
Indicine N-oxide	C[C@@H]([C@](C(C)C)(C(=O)OCC1=CC[N+]2([C@H]1[C@@H](CC2)O)[O-])O)O	[M+H]+	316.1755	172.2	173.9	169.92	1.34	2.31
		[M+H-H2O]+	298.1649	169.3	/			
		[M+Na]+	338.1575	175.6	178.3			
		[M+NH4]+	333.2021	174.9	177.0			
		[M-H]-	314.1609	179.2	179.9			
		[M+Na-2H]-	336.1429	179.8	186.5			
		[M+HCOO]-	360.1664	180.6	/			
Usaramine	CC=C1CC(C(C(=O)OCC2=CCN3C2C(CC3)OC1=O)(CO)O)C	[M+H]+	352.1755	181.9	178.9	180.89	0.56	1.1
		[M+H-H2O]+	334.1649	179.0	/			
		[M+Na]+	374.1575	185.4	182.0			
		[M+NH4]+	369.2021	184.6	188.6			
		[M-H]-	350.1609	183.4	179.2			
		[M+Na-2H]-	372.1429	183.6	172.9			
		[M+HCOO]-	396.1664	183.9	/			
Usaramine N-oxide	C/C=C/1\C[C@H]([C@@](C(=O)OCC2=CC[N+]3([C@H]2[C@@H](CC3)OC1=O)[O-])(CO)O)C	[M+H]+	368.1704	184.4	182.9	182.32	1.14	0.32
		[M+H-H2O]+	350.1598	181.7	/			
		[M+Na]+	390.1524	187.7	179.6			
		[M+NH4]+	385.1970	187.0	189.9			
		[M-H]-	366.1558	188.0	181.6			
		[M+Na-2H]-	388.1378	188.5	181.4			
		[M+HCOO]-	412.1613	189.2	/			
Spartioidine	C/C=C/1\CC(=C)[C@](C(=O)OCC2=CCN3[C@H]2[C@@H](CC3)OC1=O)(C)O	[M+H]+	334.1649	178.0	175.8	176.80	0.68	0.57
		[M+H-H2O]+	316.1543	174.8	/			
		[M+Na]+	356.1469	181.7	181.3			
		[M+NH4]+	351.1915	180.8	186.1			
		[M-H]-	332.1503	181.1	175.9			
		[M+Na-2H]-	354.1323	181.0	169.5			
		[M+HCOO]-	378.1558	181.2	/			
Integerrimine	C/C=C/1\C[C@H]([C@@](C(=O)OCC2=CCN3[C@H]2[C@@H](CC3)OC1=O)(C)O)C	[M+H]+	336.1806	178.6	176.8	178.86	0.15	1.15
		[M+H-H2O]+	318.1700	175.5	/			
		[M+Na]+	358.1626	182.3	182.4			
		[M+NH4]+	353.2072	181.4	187.2			
		[M-H]-	334.1660	182.1	177.5			
		[M+Na-2H]-	356.1480	182.2	169.9			
		[M+HCOO]-	380.1715	182.5	/			
Integerrimine N-oxide	C/C=C/1\C[C@H]([C@@](C(=O)OCC2=CC[N+]3([C@H]2[C@@H](CC3)OC1=O)[O-])(C)O)C	[M+H]+	352.1755	181.9	178.9	179.83	1.15	0.52
		[M+H-H2O]+	334.1649	179.0	/			
		[M+Na]+	374.1575	185.3	177.6			
		[M+NH4]+	369.2021	184.5	186.6			
		[M-H]-	350.1609	186.4	177.8			
		[M+Na-2H]-	372.1429	187.0	177.7			
		[M+HCOO]-	396.1664	187.7	/			
Heliosupine	C/C=C(/C)\C(=O)O[C@H]1	[M+H]+	398.2174	193.9	194.2	192.06	0.96	1.11
		[M+H-H2O]+	380.2068	191.7	/			

	CCN2[C@@H]1C(=CC2)COC(=O)[C@](C@H](C)O)(C(C)(C)O)O	[M+Na]+	420.1994	196.5	206.0			
		[M+NH4]+	415.2440	196.0	201.0			
		[M-H]-	396.2028	194.4	205.5			
		[M+Na-2H]-	418.1848	195.4	198.6			
		[M+HCOO]-	442.2083	196.6	/			

Heliosupine N-oxide	[O-][N+]12[C@]([C@H](CC2)OC(/C(C)=C\C)=O)([H])C(COC([C@@][C@@H](O)C)(O)C(C)(O)C)=O)=CC1	[M+H]+	414.2123	195.7	198.3	190.17	2.91	4.28
		[M+H-H2O]+	436.1943	200.0	/			
		[M+Na]+	431.2389	198.3	204.1			
		[M+NH4]+	396.2017	195.6	200.3			
		[M-H]-	412.1977	197.2	207.4			
		[M+Na-2H]-	434.1797	194.1	210.7			
		[M+HCOO]-	458.2032	204.1	/			
Spartioidine N-oxide	C=C1C/C(=C\C)C(=O)O[C@@H]2CC[N+]3([O-])CC=C(COC(=O)[C@]1(C)O)[C@H]23	[M+H]+	350.1598	180.3	177.9	178.27	1.14	0.21
		[M+H-H2O]+	372.1418	191.6	/			
		[M+Na]+	367.1864	189.4	176.5			
		[M+NH4]+	332.1492	177.7	185.5			
		[M-H]-	348.1452	183.9	176.3			
		[M+Na-2H]-	370.1272	185.8	177.2			
		[M+HCOO]-		191.8	/			

Figure 4.7

The black chromatogram represents Method 1 (Acetonitrile mobile phase), Method 2 (methanol mobile phase) is displayed in the red chromatograms and the green peak represents the chosen Method 8. The chromatograms substantiate the improving quality of the peaks when changing the UPLC/MS-MS conditions.

1) Improving peak shape of heliotrine

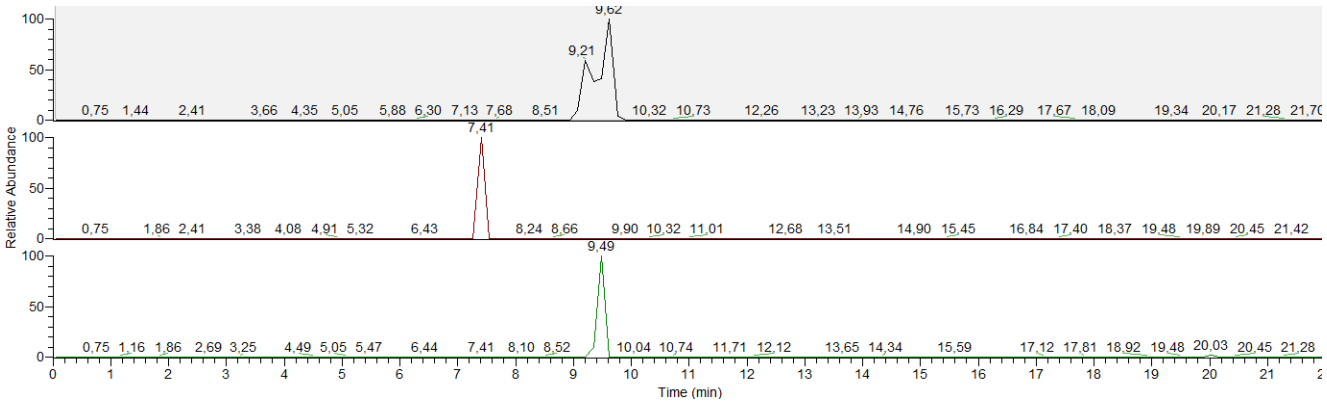

2) Improving peak shape of intermedine N-oxide and lycopsamine N-oxide. Improved separation of the compounds can be observed.

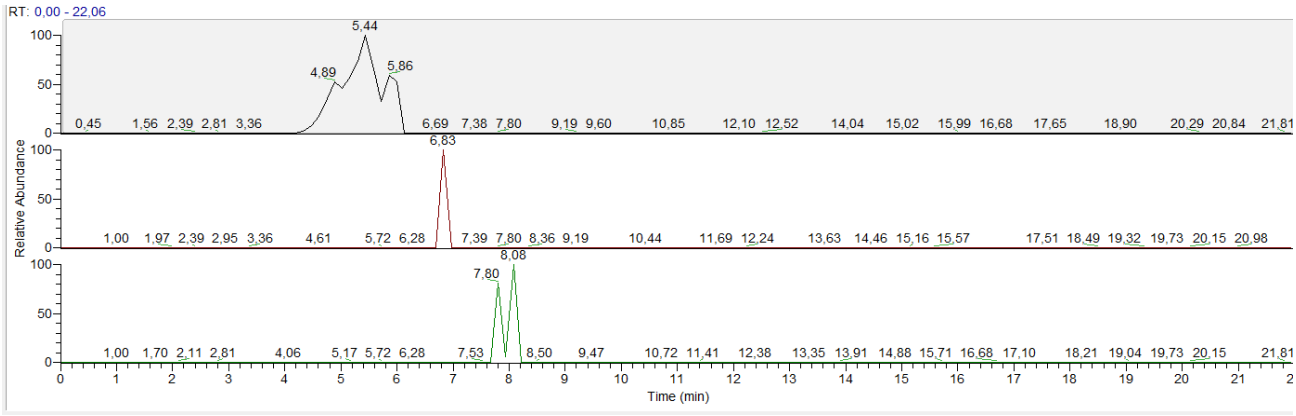

3) Improving peak shape of retrorsine N-oxide.

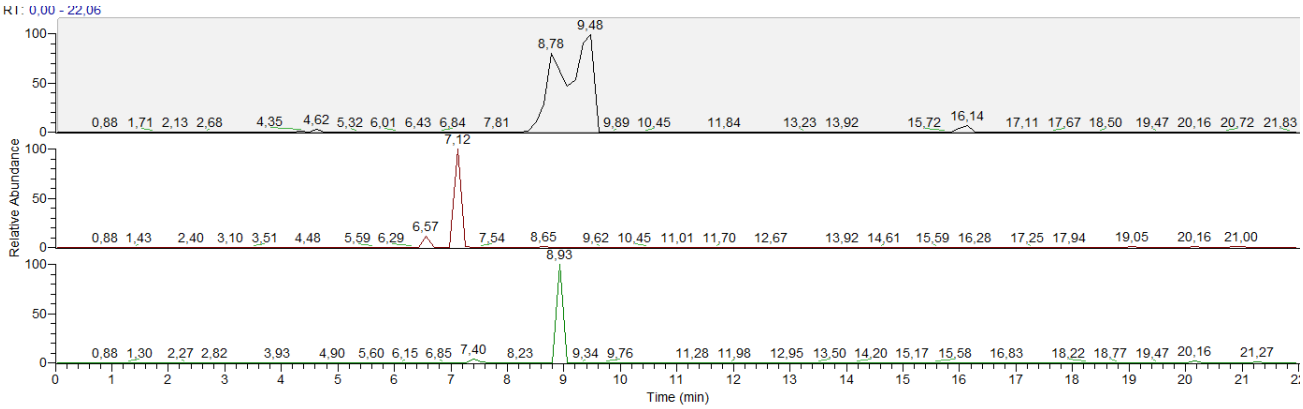

4) Improving peak shape of europine N-oxide.

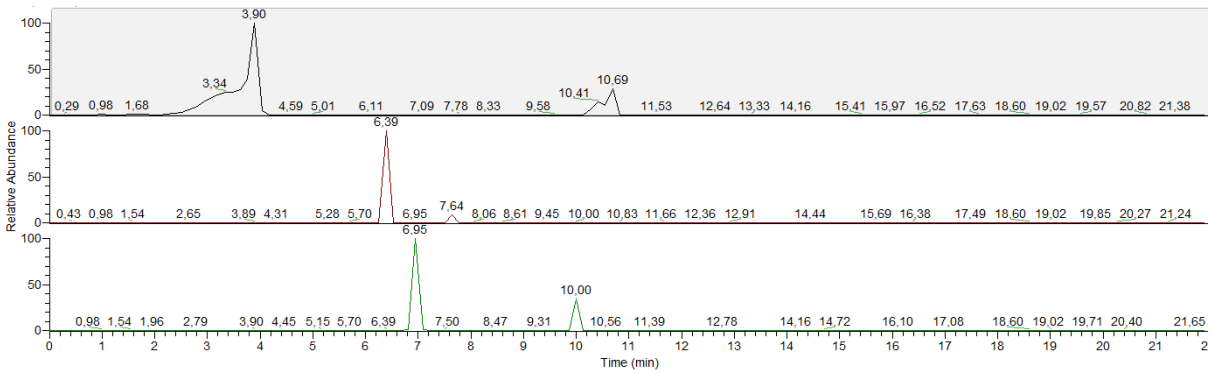

Table 4.11

***Overview of retention time, precursor ion (Q1) and fragmentations (Q3) of the most common PAs. The bold fragments are defined as quantifiers, the other fragments are qualifiers. Information was pooled from three sources, to identify the peaks from the standard mixture with more certainty. The numbers in black are obtained from* (27), *the blue values are obtained from* (26), *the green values are derived from* (67).**

Pyrrolizidine alkaloids	Retention time (min)	Q1 mass (*m/z*)	Q3 mass (*m/z*)
Echimidine (Em)	9.9 7.28	398.2 398.4	**120**, 220, 336 **120.2**, 220.2 120, 220
Echimidine N-oxide (EmN)	10.9 7.12	414.2	**254**, 352, 396 254, 352
Erucifoline (Er)	2.8 4.19	350.2	**120**, 138, 136 138, 94
Erucifoline N-oxide (ErN)	5.2 4.66	366.2	**118**, 136, 120 118, 164
Europine (Eu)	3.4 4.63	330.2	**138**, 156, 254 138, 94
Europine N-oxide (EuN)	4.9 4.91	346.2	**172**, 111, 136 172, 256
Heliotrine (Hn)	6.2 5.81	314.2 314.0 314.2	**138**, 156, 120 **138.0**, 94.1, 120.0 138, 156
Heliotrine N-oxide (HnN)	7.4 6.14	330.2	**172**, 111, 136 **172.1**, 138.2 172, 111
Intermedine (Im)	3.0 4.57	300.2 300.3	**138**, 156, 120 **138.1**, 156.1 120, 156
Intermedine N-oxide (ImN)	4.9 5.15	316.2	**172**, 138, 111 111, 172
Jacobine (Jb)	4.0 4.52	352.2	**120**, 155, 280 120, 155
Jacobine N-oxide (JbN)	6.3 4.79	368.2	**296**, 120, 324 120, 296
Lasiocarpine (Lc)	11.6 8.30	412.2	**120**, 220, 336 **120.1**, 336.2 120, 220
Lasiocarpine N-oxide (LcN)	11.9 8.62	428.2 428.3	**254**, 136, 352 **254.1**, 136.1 138, 254
Lycopsamine (La)	3.2 4.71	300.2 300.3 300.2	**138**, 156, 120 **138.1**, 156.1 94, 156
Lycopsamine N-oxide (LaN)	5.1 5.27	316.2	**172**, 138, 111 172, 94
Monocrotaline (Mc)	1.6 3.48	326.2	**120**, 237, 194 120, 194

Monocrotaline N-oxide (McN)	3.8 5.53	342.2 342.1	**137**, 118, 120 **137**, 119.1, 236.1 120, 138
Retrorsine (Re)	6.0 5.50	352.2 352.0	**120**, 138, 324 **120**, 138, 324.1 138, 324
Retrorsine N-oxide (ReN)	7.5 5.58	368.2	**118**, 120, 136 120, 136
Seneciphylline (Sp)	6.5 5.73	334.2	**120**, 136, 306,138 **120, 94.1, 138, 118** 138, 306
Seneciphylline N-oxide (SpN)	8.3 5.92	350.2	**120**, 118, 136 **118.2**, 136.2, 138.2, 306.1, 95, 118
Senecivernine (Sv)	7.9	336.2	**120**, 138, 308
Senecivernine N-oxide (SvN)	9.6	352.2	**118,** 120 136
Trichodesmine (Td)	5.8	354.2	**120**, 138, 308 **222.2**, 120.2
Senecionine (Sc)	8.2 6.48	336.2	**120**, 138, 308 **120**, 94.1, 138 94, 308
Senecionine N-oxide	9.8 6.6	352.2	**118,** 120, 136 **120**, 118, 138, 324 118, 220
Senkirkine (Sk)	9.7 7.49	366.2	**168**, 150, 122 122, 168

Master dissertation submitted to the faculty of Pharmaceutical Sciences, performed in collaboration with the Laboratory Food and Drug

Promotor: Prof. Dr. Chiara Dall'Asta

Second promotor: Prof. Dr. Marthe De Boevre

Commissioners: Dr. Agustina Pavicich and Dr. Amina Badmos

This master dissertation is an examination document that not necessarily has been corrected for eventual mistakes. The information, conclusions and points of view in this master dissertation are those of the author and do not necessarily represent the opinion of the promoter or his/her research group.